

## Rubberized geopolymmer composites: A comprehensive review

Shaker M.A. Qaidi<sup>a</sup>, Ahmed S. Mohammed<sup>b,\*</sup>, Hemn Unis Ahmed<sup>b</sup>, Rabar H. Faraj<sup>c</sup>, Wael Emad<sup>d</sup>, Bassam A. Tayeh<sup>e</sup>, Fadi Althoey<sup>f</sup>, Osama Zaid<sup>g</sup>, Nadhim Hamah Sor<sup>h</sup>

<sup>a</sup> Department of Civil Engineering, College of Engineering, University of Duhok, Duhok, Kurdistan Region, Iraq

<sup>b</sup> Civil Engineering Department, College of Engineering, University of Sulaimani, Sulaimaniyah, Kurdistan Region, Iraq

<sup>c</sup> Civil Engineering Department, University of Halabja, Halabja, Kurdistan Region, Iraq

<sup>d</sup> Department of Civil Engineering, Komar University of Science and Technology, Kurdistan-Region, Iraq

<sup>e</sup> Civil Engineering Department, Faculty of Engineering, Islamic University of Gaza, P.O. Box 108, Gaza Strip, Palestine

<sup>f</sup> Department of Civil Engineering, College of Engineering, Najran University, Najran, 1988, Saudi Arabia

<sup>g</sup> Department of Structure Engineering, Military College of Engineering (MCE), National University of Sciences and Technology (NUST), H-12 Campus, 44000, Islamabad, Pakistan

<sup>h</sup> Civil Engineering Department, University of Garmian, Kalar, Kurdistan Region, Iraq



### ARTICLE INFO

#### Keywords:

Rubberized geopolymers  
Waste rubber tires  
Crumb rubber  
Mechanical and durability properties  
Applications  
Embodied CO<sub>2</sub> emissions

### ABSTRACT

The construction sector has been addressing the issue of integrating sustainability into production processes over the last few years, either through solid waste materials as aggregates in concrete or the search for more eco-friendly raw materials. Besides, the global trends group focused on developing an alternative to cement, which is a significant contributor to pollution of the environment due to its greenhouse gas emissions. Geopolymer (GP) is one of the most acceptable solutions for utilizing all industrial by-products containing an aluminosilicate (A-S) source material. However, one method to recycle waste rubber tires is incorporating them into geopolymers concrete (GPC) as an alternative to natural aggregates. Recently, the potential of combining the advantages of GPC with rubberized concrete to produce rubberized geopolymers concrete (Ru-GPC) as a viable, sustainable building material has been recognized. This paper presents a state-of-the-art review of the waste rubber's environmental and economic impact, resources, recycling, classifications, and physicochemical properties. Besides, this article provides in-depth studies on the behaviors and properties of Ru-GPC composites, such as their basic components, preparation and curing processes, fresh and physical properties, mechanical properties, dynamic properties, durability properties, microstructures, and insulation properties. The effect of crumb rubber (CRu) substitution on critical properties is addressed critically. Also, it highlights the applications, embodied CO<sub>2</sub> emissions, and cost analysis of Ru-GPC. Moreover, gaps in the literature and recommendations for future study have been identified to support further developments in the investigation and future publication of Ru-GPC materials in practice.

### 1. Introduction

The disposal of waste rubber tires has become a significant environmental concern globally. Tires are continuously disposed of, discarded, or buried worldwide, posing a severe environmental threat [1, 2]. Every year, it is estimated that nearly a billion tires reach the end of their useful life, with over half being disposed of in landfills or as garbage without treatment [3,4].

As per a World Bank report (2018) [5], worldwide waste generation is expected to rise by 70% in the next thirty years to 3.5 thousand million tonnes. If the USA situation is considered, the Rubber Manufacturers

Association [6] reports that over 230 million waste rubber tires are produced each year, and over 75 million are preserved. This massive volume of non-biodegradable garbage consumes considerable land and poses environmental hazards. Thus, discarded tires are now recycled to benefit the environment and the economy to meet growing ecological concerns, as seen in Figs. 1 and 2. As per a report by the U.S.-RMA [6], just 16% of discarded tires are dumped in landfills, with the rest recycled in other ways.

Moreover, energy recovered from waste tires benefits industrial economies in developed countries. About 2%–8% of waste tires in the USA and the EU, as shown in Figs. 1 and 2 are recycled as engineering and construction materials [7].

\* Corresponding author.

E-mail address: [ahmed.mohammed@univsul.edu.iq](mailto:ahmed.mohammed@univsul.edu.iq) (A.S. Mohammed).

List of abbreviations	
GP	Geopolymer
GPC	Geopolymer concrete
CRu	Crumb rubber
Ru-GPC	Rubberized geopolymers concrete
PC	Portland cement
Sodium silicate	$\text{Na}_2\text{SiO}_3$
Sodium hydroxide	NaOH
SS/SH	Sodium silicate ( $\text{Na}_2\text{SiO}_3$ )/Sodium hydroxide (NaOH)
A-S	Alumino-silicates
AAS	Alkaline-activator solution
MOE	Modulus of elasticity
RTSF	Recycled tire steel fiber
NRC	Noise reduction coefficient
ELT	End of life tires

Tires are disposed of in many ways, including landfill disposal, burning, using as fuel, pyrolysis, and producing carbon black. Moreover, stored tires pose various health, ecological, and economic problems due to air, water, and soil pollution [8–10]. Over several years, the building industry has responded to integrating sustainability into manufacturing processes by utilizing solid waste products as aggregates in concrete or by seeking out more ecologically friendly raw ingredients [11,12]. One possible method of recycling discarded tire rubber is to include it in concrete in place of natural aggregates. This strategy can be ecologically friendly since it contributes to preventing environmental pollution caused by the disposal of discarded tires.

Moreover, it reduces carbon dioxide emissions by preventing tire fires. Consequently, rubberized concrete has garnered considerable interest as a viable technology for construction materials that may contribute to the reduction of environmental dangers. Numerous previous research shows that concrete, including CRu's, increases impact resistance while decreasing compression and flexural strengths. There is widespread agreement on the drastic drop in mechanical characteristics caused by an increase in rubber content [12–14].

Portland cement (PC) is an effective construction material. Yet, its manufacture is energy-intensive (requiring kiln temperatures of 1450–1550 °C) and has other significant ecological impacts. With approximately one tonne of CO<sub>2</sub> produced for every tonne of PC produced, this binder is a major contributor to climate change (responsible for around 7% of world emissions of CO<sub>2</sub>). Moreover, PC manufacture

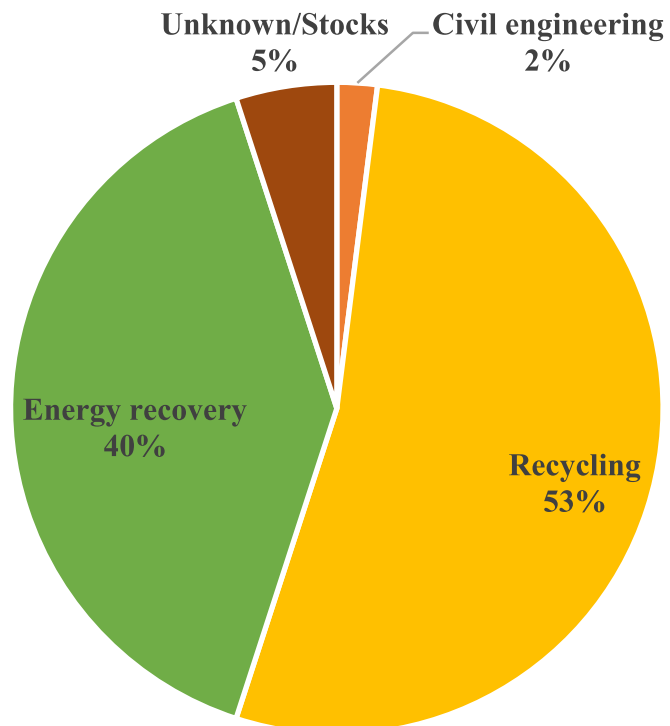


Fig. 2. Recovery of scrap tire materials in the EU (2019) [21,26].

involves extensive overuse of natural resources, mostly limestone quarries. The globe consumes more than 3 thousand million tonnes of raw materials (of which 70% are limestone) to make just 2 thousand million tonnes of PC. All of the above parameters contribute to the research and emergence of new alternative materials that are more energy-efficient and environmentally friendly (lower CO<sub>2</sub> emissions, recycling of industrial waste) while keeping or surpassing the effectiveness of ordinary PC [15–17].

Compared to PC-concrete, geopolymers concrete (GPC) has been made because it has better mechanical properties, low creep, low shrinkage, and better acid resistance [18,19]. It has also been made because it is more environmentally friendly than PC-concrete. GP adhesive binds loose fine aggregates, coarse aggregates, and other unreacted materials together [20–22]. It is an alkali-activated binder created through polymerization involving alkaline liquids, silicon, and aluminum oxides found in various kinds of raw materials. Numerous

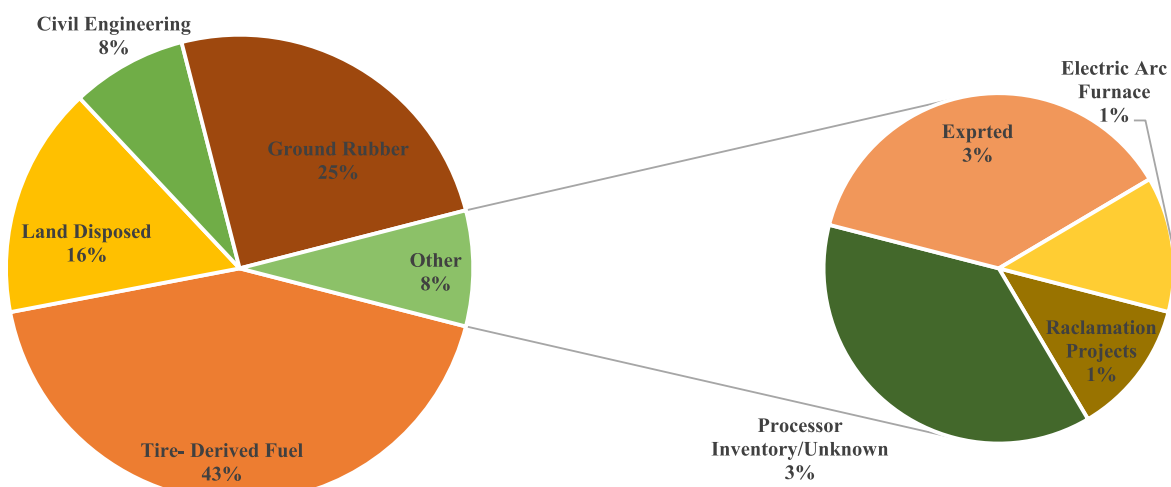


Fig. 1. Waste tire disposal in the USA (2017) [21,25].

geologically originated minerals, including metakaolin, and industrial wastes, including fly ash and ground granulated blast-furnace slag (GGBFS), can be activated [23]. As a result, it emits less CO<sub>2</sub> than PC and generates high-value construction materials by recycling industrial waste with an alumino-silicate composition [24]. Fig. 3 shows, in simplified form, the geopolymserisation process.

Limited research has been undertaken on the effect of CRu on GP concrete mixes. However, it has gained considerable attention in engineering materials due to the numerous experimental studies performed in the published studies. Additionally, the rubber content has an important impact on rubberized concrete's compressive and tensile strengths. Nevertheless, the limited available data on the mechanical characteristics of Ru-GPC tends to leave some questions unanswered, and extra-scientific facts are required to confirm the capability of producing Ru-GPC composites with CRu serving as a partial substitute for both fine and coarse aggregates. It is critical to develop rubberized concrete to meet the demand for high-performance, cost-effective, and environmentally friendly materials in contemporary construction. This paper presents a state-of-the-art review of the technical and production properties of the recent advances and perspectives of Ru-GPC.

## 2. Waste rubber

### 2.1. Disposal of waste rubber tires

Waste tire disposal has become a serious environmental concern in all countries worldwide. It is predicted that 1.5 billion tires are made each year globally [2,28,29]. Annually, millions of tires are dumped, thrown away, or buried worldwide, posing a severe danger to the environment. Tires are disposed of in many ways, including landfill disposal, usage as fuel, burning, and pyrolysis to make carbon black. Stockpiled tires also pose various health, economic, and environmental problems due to water contamination, air, and soil [9]. Because of their unique shape and waterproof nature, tires can hold water for a long time, making them a good place for mosquitoes and other pests to live and breed [30,31].

The economics of using tire rubber as fuel are unattractive.

Compared to carbon black made from petroleum sources, carbon black created from tires is more costly and of inferior quality. Tire rubber can be used in a variety of civil and non-civil engineering fields, including road construction, geotechnical work, onshore and offshore breakwaters, agriculture to seal silos, retaining walls in harbors and estuaries to cushion the impact of ships, artificial reefs to improve fishing, as a fuel in cement kilns, combustion for power generation, reefs in marine environments, and as an aggregate in cement-based products. Regardless, millions of tires are discarded, buried, or burned every year [32].

Tire burning, the cheapest and simplest form of disposal, creates major fire dangers [33]. The temperature increases in that region and the noxious smoke from uncontrolled releases of potentially harmful substances are hazardous to people, animals, and plants. Tires are made using petrochemical feedstocks like butadiene and styrene. Butadiene is a highly carcinogenic four-carbon molecule that may be generated while burning the styrene-butadiene polymer ([bur-ningissues.org](http://bur-ningissues.org)). Tire combustion emits styrene and various benzene derivatives. The contaminants in the air generate thick black smoke, which reduces vision and soil painted surfaces. Polyaromatic hydrocarbons, CO, NO<sub>2</sub>, HCl, and SO<sub>2</sub>, are among the hazardous gases emitted. The powder residue left behind after burning pollutes the earth. The problem with pyrolysis is that it makes carbon black powder, making the environment dirty.

For some years, the construction sector has focused on the issue of incorporating sustainability into its production processes, whether via the use of more environmentally friendly raw materials or the use of solid waste products as aggregates in concrete [34]. One potential use of discarded tire rubber is to include it in cement concrete to substitute for some natural particles. This attempt could be environmentally benign since it contributes to the disposal of waste tires and prevents environmental contamination. Furthermore, it contributes to carbon dioxide reduction by preventing tire fires. This procedure is also a good deal because it can save some more expensive natural aggregates [35–37].

### 2.2. Environmental and economic impact

Apart from human activities, the growth in waste disposal has opened a Pandora's Box for waste management at the end of life,

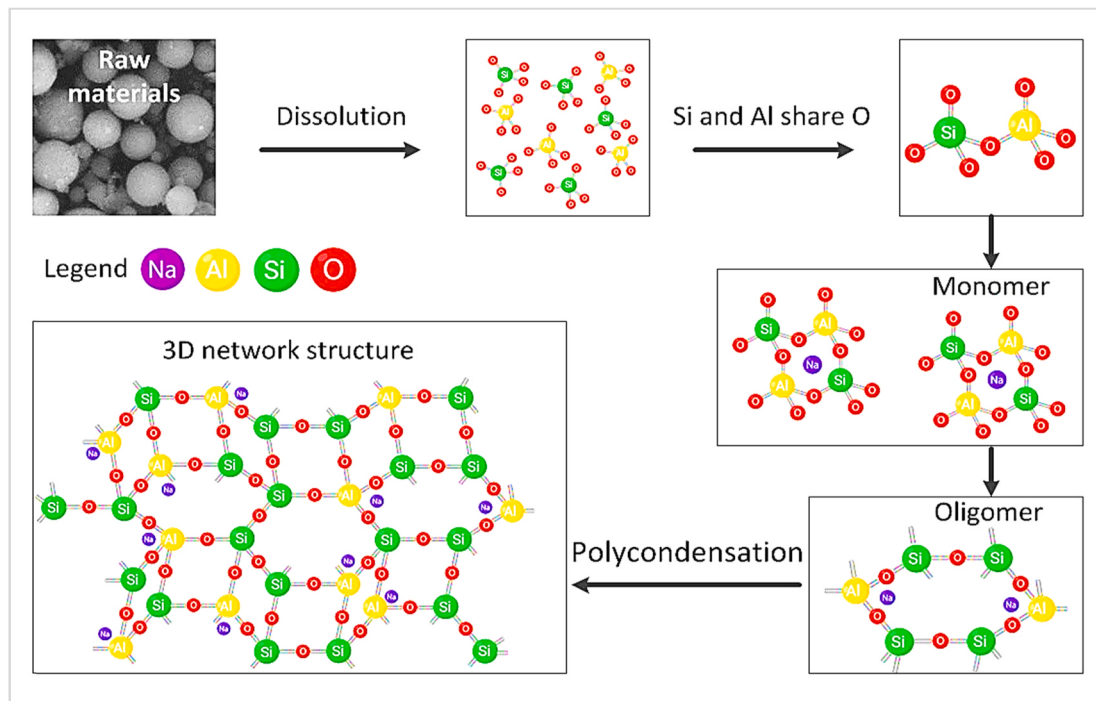


Fig. 3. Simplified geopolymserisation process [27].

encouraging worldwide academics to produce optimal waste recycling and disposal solutions that promote environmental and economic sustainability [38–43]. Among the other types of waste, end-of-life tires (ELTs) are one of the most frequent volume and shape [44,45]. Employed tires could be recycled or disposed of. ELT waste could be disposed of in landfills, thermally processed to generate energy (through incineration), or recycled to get raw ingredients [46–48]. The first two techniques (disposal and incineration) could cause various ecological issues regarding waste tire management. For instance, during landfill disposal, this could function as a breeding site for disease-carrying insects and rodents, or it could be a product of dioxins and other high volatility toxins during incineration, posing serious health risks [49,50]. As a result of these aspects, rubber tires are treated selectively to produce granules, flakes, powders, and textiles, enabling them to be employed in several sophisticated applications, including concrete [46, 51,52].

The ecological benefits of utilizing rubber in concrete include the proper disposal of dumped and non-biodegradable rubber tires, road infrastructure water resistance, decreased demand for natural raw material supply, elimination of the need for capital assets, and, therefore, a contribution to sustainable management [53–55]. Because of the amount of fine and coarse materials used in building, including rubber in concrete, it can effectively help conserve the ecosystem while also minimizing building costs [56–58].

Recycling waste in any form is beneficial. Academics have spent decades attempting to find an adequate standard for recycling tire waste using a variety of approaches. The global tire recycling market was worth \$4.54 billion in 2021 and is predicted to reach \$5.38 billion by 2026, increasing at a cumulative annual growth rate of 3.41% throughout the forecast timeframe, as shown in Fig. 4-a. If the USA scenario is taken into account, the US tire recycling market was worth \$0.89 billion in 2015 and is predicted to reach \$1.15 billion by 2031, increasing at a cumulative annual growth rate of 2.6% throughout the forecast timeframe, as shown in Fig. 4-b [59].

### 2.3. Resources

Tires are the primary source of CRu, which is broadly classified as truck and vehicle tires [60]. The physical and chemical characteristics of tires vary depending on their origin [61]. As a result, the influence on concrete strength differs. While tires are typically comprised of a unique combination of materials, they are toughened to obtain the appropriate properties. Yet, most of them have nearly the same volume of rubber [25]. Fig. 5 shows a typical tire structure, and Table 1 lists the most important parts of each tire.

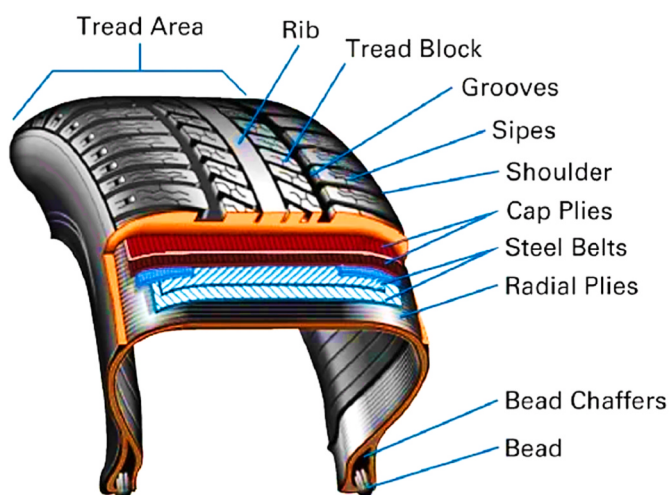


Fig. 5. Tire structure and engineered layers [62].

### 2.4. Recycling

Tire waste is typically utilized for energy recovery, and various types of waste-derived automobiles are also recovered in the building industry [25,66]. The methods of waste tire recycling vary based on the goals. Waste tires have enormous potential as a material for construction since they include steel, fibers, and rubber, all of which can be recovered using various techniques [25]. As concrete additives, steel and fibers can be used [67]. CRu, on the other hand, can be utilized as a coarse or fine aggregate [25]. At the same time, rubber powder can be used as a filler or binder in concrete [60,68]. This study focuses on studying the different properties of CRu in the form of aggregate. Fig. 6 illustrates the fundamental processing steps for a waste rubber recycling plant, which can be divided into three major steps: crushing and grinding screening, and magnetic separation [69]. This provides a framework for further inspections.

### 2.5. Classifications and physico-chemical properties

Earlier studies categorized the waste rubber used in concrete into distinct categories based on its size. Table 2 and Fig. 7 show the standard rubber divisions and sizes.

The physical properties of tires differ considerably based on the source. Consequently, when used, they have varying effects on the

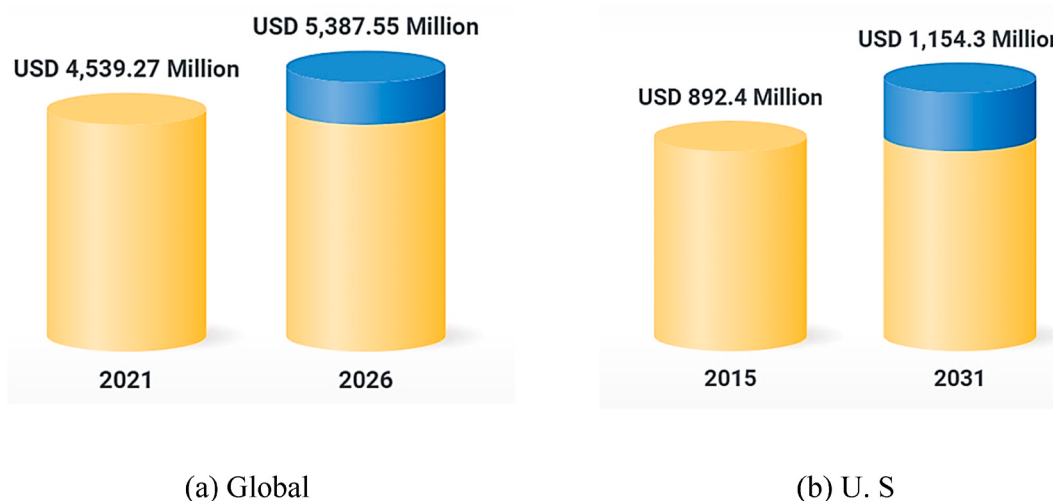
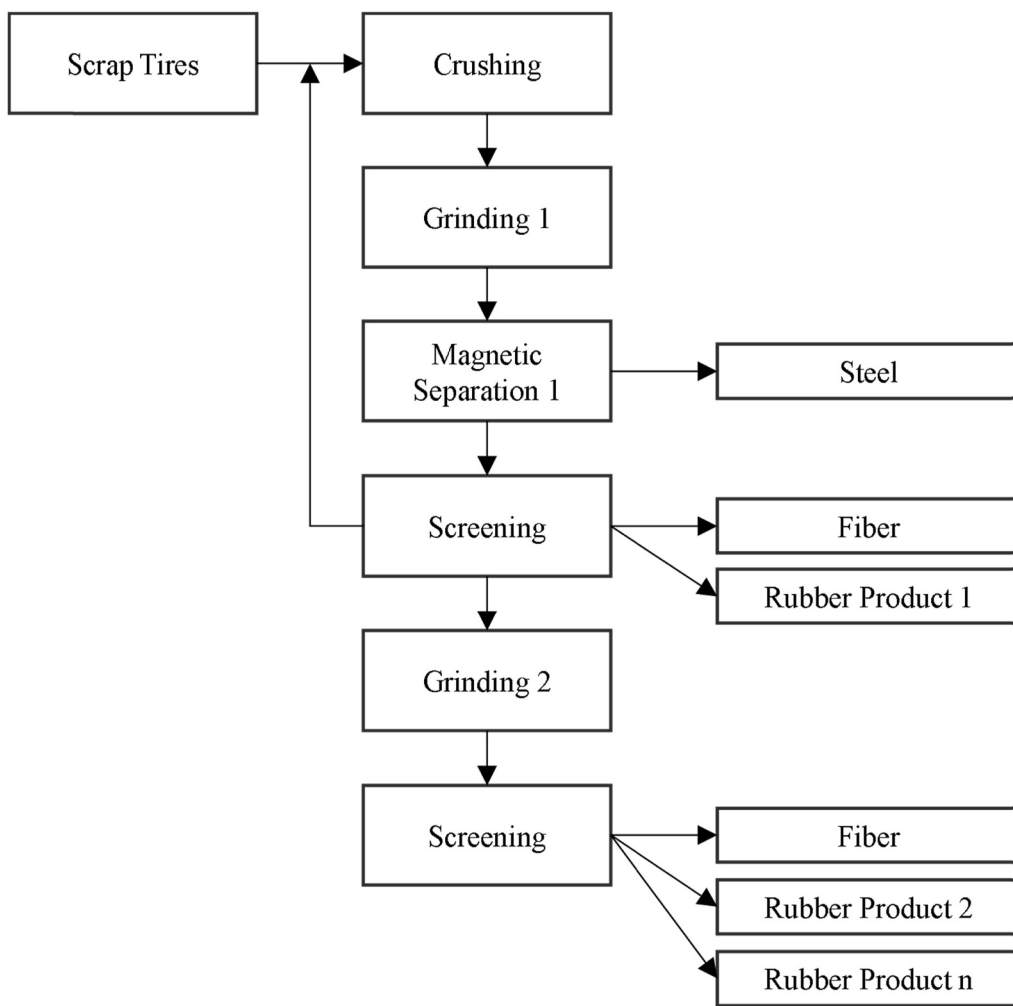


Fig. 4. Tire recycling downstream products market: (a) global, and (b) U.S [59].

**Table 1**  
Compositions of a standard tire.

Type of tire	Compositions (%)						Ref.
	Synthetic rubber	Natural rubber	Carbon black	Ash	Steel	Others	
Car tire	–	43–48	20–28	–	14–16	3–6	[63]
	45–55	22–42	30–38	2–7	–	–	[64]
	26	15	28	–	13–15	–	[65]
Truck tire	15	26	28	–	14.5–15	–	[64]
	–	42–45	21–28	–	21–27	1–10	[65]



**Fig. 6.** The fundamental phases of producing a waste tire recycling plant [69].

**Table 2**  
Rubber aggregate classifications.

Aggregates size (mm)				Ref.
Powdered/ground rubber	CRu	Shredded/chipped rubber	Fiber rubber	
0.075–0.0475	0.425–4.75	11–76	–	[68]
0.15–19	0.5–5.0	12–76	8.5–21.5	[83]
<1	3–10	25–30	–	[60]

strength of concrete [25]. Synthetic and biological rubber, metal, carbon black, fabric, and additives are common tire elements [25]. Incorporating various additives into tire rubber products, such as antioxidants, stabilizers, and antiozonants, makes them non-biodegradable, impermeable to chemical reagents, photochemical degradation, and high

temperatures [63]. The chemical composition of CRu, on the other hand, changes, as do the physical properties, based on the methods of manufacture of tires and the origins of the basic materials [70]. CRu particles have a specific gravity ranging from 1.05 to 1.15 [71–73]. Li, Li, Wei, Zhang, Wei and Li [74], CRu particles have a bulk density of 260–460 kg/m<sup>3</sup>. Also, many investigations have found that the melting point of CRu is about 170 °C [75–77]. Moreover, CRu is a hydrophobic material with a considerable water contact angle, varying from 95° to 122° [78–81]. When additional CRu was added to concrete, Akinyele, Salim and Kupolati [82] noticed a decrease in the amount of key components, including Ca, Fe, Si, O, and Al. Furthermore, as expected, the amount of S and C in the mixture rose as the amount of CRu increased, due to the elevated sulfur and carbon black content of tire rubber [82]. The physical and chemical properties of the CRu's are shown in Tables 3 and 4.

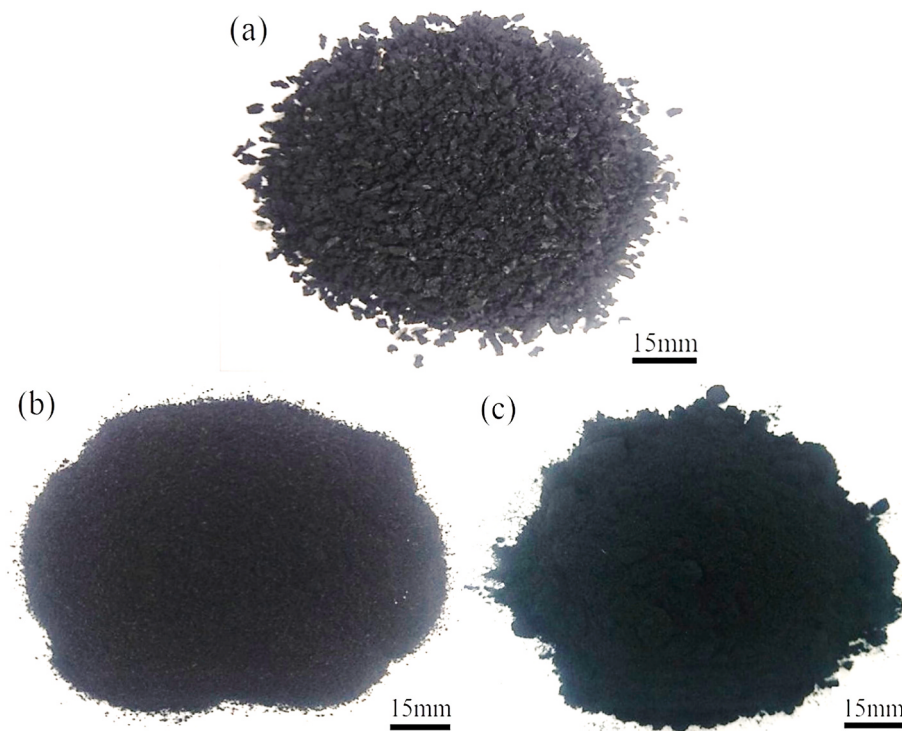


**Fig. 7.** Different sizes of CRu particles: (a) 2 mm, (b) 750  $\mu\text{m}$ , and (c) 375  $\mu\text{m}$  [84].

**Table 3**  
Physical properties of the CRu.

Size (mm)	property	Ref.
0.15–2.36	Water absorption (%)	0.84
2–6	0.65	535 [85]
0–5	/	1.13 [86]
5–10	/	410–465 [87]
10–20	5.30–8.90	1.12
	0.80–1.30	460
		485

### 3. Main material of rubberized geopolymer concrete

#### 3.1. Alumino-silicates (A-S)

GGBFS, fly ash, metakaolin, silica fume, rice husk ash, red mud, and waste wood ash are common A-S precursors employed in the production of GP concrete. When these materials are combined with an alkaline liquid, they release silica and aluminum, leading to GP gels [94]. Raw materials' mineralogical and chemical composition significantly impacts their reactivity [21]. Table 7 presents the A-S source materials utilized in various research to make rubberized alkali-activated concrete, revealing that most studies employed GGBFS, or fly ash, and

**Table 4**  
Chemical composition of the CRu.

Composition (%)											Ref.	
Carbon Black	Oxygen	Zinc	Sulfur	Silicon	Polymer	Magnesium	Aluminum	Nitrogen	Ash	Hydrogen	Organic compounds	
87.52	9.23	1.76	1.09	0.20	/	0.14	0.08	/	/	/	/	[88]
91.50	3.3	3.5	1.20	/	/	/	/	/	/	/	/	[89]
81.2–85.3	1.72–2.07	/	1.32–1.64	/	/	/	/	0.32–0.47	/	7.22–7.43	/	[90]
40.1	/	/	/	45	/	/	/	/	/	/	15	[91]
30–39	/	/	1–5	/	42–55	/	/	/	3–71	/	/	[92]
31.35	/	/	3.24	/	38.3	/	/	/	5.44	/	/	[93]

**Table 5**  
Chemical composition of GGBFS.

Chemical composition (%)													Refs.	
SiO <sub>2</sub>	Al <sub>2</sub> O <sub>3</sub>	Fe <sub>2</sub> O <sub>3</sub>	MnO	MgO	Na <sub>2</sub> O	SO <sub>3</sub>	CaO	K <sub>2</sub> O	P <sub>2</sub> O <sub>5</sub>	TiO <sub>2</sub>	CL	SrO	LOI	
34.10	12.30	0.41	0.25	8.12	/	2.59	44.20	0.56	/	0.96	/	/	/	[95]
36.95	10.01	1.48	0.52	6.43	1.39	3.52	33.07	0.74	0.10	0.52	0.05	/	/	[96]
31.40	13.10	0.80	0.20	5.50	0.30	4.00	43.20	0.30	0	0.60	/	/	0.60	[97]
32.92	13.80	0.58	/	5.76	0.20	3.33	42.13	0.32	0.034	0.57	/	/	/	[98]
34.95	13.58	0.53	0.15	3.58	0.26	2.52	42.88	0.61	/	0.63	/	/	/	[99]
35.12	14.20	0.62	0.69	8.47	0.98	/	39.08	/	/	0.71	/	/	0.13	[100]
36.10	9.30	0.03	/	8.90	0.80	2.20	39.00	0.60	/	/	/	/	1.01	[101]

**Table 6**  
Chemical composition of fly ash.

	Chemical composition (%)													Refs.
	SiO <sub>2</sub>	Al <sub>2</sub> O <sub>3</sub>	Fe <sub>2</sub> O <sub>3</sub>	MnO	MgO	Na <sub>2</sub> O	SO <sub>3</sub>	CaO	K <sub>2</sub> O	P <sub>2</sub> O <sub>5</sub>	TiO <sub>2</sub>	CL	SrO	LOI
Class F fly ash	54.70	29.00	6.74	/	0.80	1.88	0.10	1.29	/	/	/	/	/	2.72
	55.90	27.80	7.09	/	/	/	/	3.95	1.55	/	2.25	/	0.37	/
	50.00	23.40	17.29	0.22	/	/	0.08	5.06	1.41	/	1.60	/	/	[103]
	50.40	31.50	10.40	/	1.10	0.30	0.10	3.30	0.50	0.50	1.90	/	<0.1	[104]
	50.30	22.90	8.17	0.08	2.00	/	0.58	3.38	3.55	/	1.15	/	/	[98]
	61.75	24.61	6.47	/	1.53	/	/	3.45	0.55	/	0.91	/	/	[95]
	55.90	23.90	7.90	0.10	1.30	0.40	0.30	7.00	1.00	0.50	1.30	/	/	0.30
Class C fly ash	39.40	20.80	11.50	/	2.20	1.40	4.20	14.5	2.40	0.20	0.50	/	/	1.50
	50.67	18.96	6.35	/	3.12	0.69	0.74	14.14	/	/	/	/	/	0.17
	45.85	16.82	12.05	0.18	2.90	0.50	3.76	12.97	1.83	0.28	0.48	/	0.05	/

**Table 7**  
Summary of previous studies for precursor, alkaline-activator, admixture, and curing methods.

Precursors	Alkaline activators			Admixtures			Curing			Temps. (°C)	Refs.
	Na <sub>2</sub> SiO <sub>3</sub> (modulus of silicate)	NaOH (molarity)	SS/SH	AA/AP	Type	Doses (SP/AP)	Type	Duration (hrs)			
Class C fly ash	2.41	10, 15, 20	0.51	0.650	/	/	Oven	48	25	[98]	
			1.5	0.750					60		
				0.85					90		
	2.41	10	1	0.75	/	/	Oven	48	60	[140]	
	1.85	12	N.M	N.M	/	/	Heat	6	60	[108]	
	2.15	6, 8, 10, 12	0.33	0.6	/	/	Ambi.	U.T	25	[119]	
	2.5	8, 14	0.52	N.M	PB	N.M	Steam	7-d	46	[102]	
Class C fly ash + Class F fly ash	3.2	12	2.0	0.40	/	/	Ambi.	U.T	20–22	[104]	
	2.0	14	2.5	0.4	NB	2%	Oven	48	90	[118]	
	N.M	14	2.5	0.4	NB	2%	Oven	48	90	[121]	
Class F fly ash + GGBFS	N.M	10	N.M	0.45	NB	2%	Hot water curing	48	60	[124]	
	N.M	12	2.5	0.5	/	/	Seawater	U.T	N.M	[103]	
	N.M	10	2	0.4	/	/	Ambi.	U.T	20–22	[123]	
	N.M	10, 12, 14	1.52	0.30	NB	2%3%4%	Oven	24, 48, 72	60, 75, 90	[129]	
				2.5	0.350	0.4					
	N.M	8	2.5	0.45	NB	2%	Oven	24	60	[141]	
Class F fly ash + GGBFS	2.0	10	2.0	0.4	PB	1%	Ambi.	U.T	20 ± 2	[95]	
	3.2	14	2.5	0.4	PB + VMS + setting time retarder	5.55 mL/kg 5.55 mL/kg 11.12 mL/kg	Ambi.	U.T	23	[98]	
Class F fly ash + PC	2.3	12	1.58	0.37	/	/	Ambi.	U.T	25 ± 5	[106]	
	2.0	12	1.5	0.4	/	/	Oven	48	80	[105]	
Class F fly ash + Waste wood ash fly ash	N.M	12	2.5	0.4	Super lubricant	1.5%	Oven + Ambi.	48 Until the test	60 N.M	[120]	
fly ash + GGBFS	N.M	10	2.5	0.80	/	/	N.M	N.M	N.M	[142]	
	N.M	10, 12, 14	1.52	0.30	NB	2%3%4%	Oven	24, 48, 72	60, 75, 90	[128]	
			2.5	0.35	0.4						
	N.M	12	N.M	N.M	/	/	Ambi.	U.T	N.M	[98]	
	N.M	12	2.5	0.6	/	/	N.M	N.M	N.M	[122]	
GGBFS + Calcium hydroxide	GGBFS	0.39	0.54	/	/	/	Ambi.	U.T	N.M	[116]	
	3.39	/	0.3	/	/	/	Heat curing	28-d	45 ± 1	[96]	
	1.96	N.M	6.13	0.152	/	/	Ambi.	U.T	20 ± 2	[100]	
	2.6	10	0.69	0.6	PB	1%	Ambi.	U.T	23 ± 2	[126]	
	2.6	10	0.69	0.58	/	/	Ambi.	U.T	N.M	[101]	
Metakaolin	/	/	/	/	PB defoamer	2.7%, 3.6%, 5%, 2.9% 0.1%	Water	U.T	23 ± 3	[99]	
	N.M	15	2.9	0.84	/	/	Oven	48	65	[117]	

U.T = Until testing, NB = naphthalene-based, PB = polycarboxylate-based, SP = superplasticizer, VMA = viscosity modifying agent, N.M. = Not mention.

frequently the two in combination. Tables 5 and 6 show the chemical compositions of GGBFS and fly ash utilized in various research to obtain rubberized concrete.

### 3.2. Alkaline-activator solution (AAS)

As demonstrated in Table 7, sodium hydroxide and sodium hydroxide were utilized as AAS in rubberized concrete. GP concrete can also be

made using potassium silicate and potassium hydroxide [109]. These alkaline liquids aid in extracting aluminum oxide and silicon dioxide from source material A-S to create GP binders [110] and are normally made one day before blending [102]. As shown in Table 7, the molarity of sodium hydroxide solutions employed in rubberized concrete mixtures ranged from 6 molarity [111] to 20 molarity [107]. The molarity of sodium hydroxide solution affects the compressive strength of rubberized concrete and GP concrete mixtures [112,113]. High doses of sodium hydroxide have a negative impact on mechanical characteristics [114,115], although this relies on the precursor materials, such as reactivity, fineness, and chemical composition [108]. Conversely, sodium hydroxide, frequently referred to as water glass, is employed in various industrial and commercial uses and can be manufactured in highly viscous or solid conditions [116]. As indicated in Table 7, numerous research on rubberized concrete employed sodium hydroxide with a modulus of silicate varying from 1.86 [108] to 4.50 [117], with ideal values ranging from 2.0 to 2.50 [95,105,106,118]. The SS/SH ratio determines the characteristics of GP concrete [105]. In the investigations on rubberized concrete included in Table 7, the SS/SH ratio ranged from 0.33 [119] to 2.90 [117], although most of the investigations used a ratio between 1.50 and 2.50 [118,120–122]. Aside from the molarity of the SS/SH ratio and the sodium hydroxide solution, the ratio of AAS to A-S precursor, which ranged between 0.15 [100] and 0.85 [107] in rubberized concrete investigations, with an optimal value of 0.40 [98,123].

### 3.3. Natural aggregates

Aggregates are often classified as coarse aggregates or fine aggregates based on their size. Table 7 shows the type, size, proportion, and specific gravity of the coarse aggregates and fine aggregates utilized in the production of rubberized concrete. Coarse aggregate was obtained from a variety of resources, including crushed gravel [124], crushed dolomite [116], crushed basalt [116], and lightweight coarse aggregates [125]. Natural sand was the most prominent source utilized by fine aggregates. Fine aggregates typically account for 30–45% of natural aggregates by mass, with coarse aggregates accounting for the rest. Fine aggregates consist entirely of aggregates in rubberized GP mortar [107, 111,126].

### 3.4. Rubber particles

Rubber particles recycled from discarded tires substitute for a proportion of fine, coarse, or total natural aggregate in rubberized concrete [127]. Because of their larger size, shredded rubber particles are usually utilized as alternative coarse aggregates in concrete, whereas CRu particles are frequently utilized as alternative fine aggregates. Even though extremely fine ground rubber (powdered) has been utilized to substitute the binder in rubberized concrete partially, powdered rubber lacks cementitious characteristics [96]. Table 7 shows the rubber particles' type, size, percent substitution, and specific gravity in rubberized concrete. Most research employed CRu to substitute natural aggregates, whereas just a few used rubber fibers [128,129] and natural rubber latex [119]. The substitution of natural aggregates in rubberized concrete by CRu particles was up to 100% [107], resulting in strengths sufficient for rubberized concrete bricks/blocks [130]. Other research incorporated 60 vol% CRu substitution [100,126]. However, as indicated in Table 7, most investigations limited the substitution to 30 vol%.

### 3.5. Admixtures

The majority of the admixtures employed in rubberized concrete investigations were either superplasticizers or high-range water reducers. Due to GP concrete mixtures' increased alkalinity, available commercial superplasticizers were designed for PC-concrete, and applying them to GP concrete provides a challenge. They performed

poorly when certain superplasticizers were introduced to GP concrete [131–134]. Many studies explore the influence of superplasticizers on GP concrete made with GGBFS [135], fly ash [132,136,137], both fly ash and GGBFS [138] and metakaolin [139]. It was discovered that the efficiency of superplasticizers was dependent on the activator utilized, the water content, the water content, the A-S source material, and the blending circumstances. Superplasticizers based on polycarboxylates, and naphthalene were the most often utilized in rubberized concrete mixtures, as shown in Table 7. The superplasticizers used in various rubberized concrete mixtures ranged from 1% [126] to 5% of the binder content [99]. Luhar, Chaudhary and Dave [128] investigated the impact of various naphthalene sulfonate-based superplasticizer doses (2–4%) on the compressive strength of rubberized concrete and discovered that larger concentrations led to decreased compressive strength. In addition to superplasticizers, a setting time retarder [98], a viscosity modifying agent [98], and a defoamer [99] were added to rubberized concrete mixtures. A setting time aids in delaying concrete setting, while a viscosity modifying agent changes the rheology of the concrete mixture to achieve good workability.

## 4. Preparation and curing of rubberized geopolymer concrete

### 4.1. Rubber waste pretreatment

Before blending, rubber waste is pretreated to minimize the adverse effects of CRu inclusion. Pretreatment approaches for various Ru-GPC mixtures are listed in Table 7, which primarily involve water soaking/washing and sodium hydroxide pretreatment. Both approaches include immersing the rubber particles in the pretreatment liquid for approximately 60 s and then closing the container for 24 h at room temperature [106]. After draining the solution, the rubber is carefully cleaned to reduce its pH to about seven. The rubber particles are dried to achieve saturated surface dry (SSD) conditions.

Regarding soaking in water, the water is drained after 24 h s, and the rubber particles are supposed to reach an SSD state before being introduced to the mixture [98]. Both pretreatment approaches effectively eliminated contaminants from the surfaces of CRu particles [122] while keeping the same surface texture [106]. Nevertheless, compared to water soaking, pretreatment with sodium hydroxide resulted in the formation of more needle-formed crystals on the surfaces [122]. Pretreatment with a sodium hydroxide solution aids in the removal of the zinc stearate layer from the surface of the CRu particles, which acts as a barrier between both the concrete mixture and rubber [143–146]. Moreover, immersing the mixture in water can help increase compressive strength and minimize air entrapped [73].

Pham, Lim and Malekzadeh [141] studied the characteristics of four distinct CRu pretreatment regimens on the characteristics of Ru-GPC based on fly ash. Pretreatment approaches studied comprised immersing CRu particles in a sodium hydroxide solution, soaking in water, coating CRu particles with ultra-fine slag, or coating CRu particles with cement paste. As demonstrated by the results, all pretreatment approaches improved compressive strength [141]. When compressive strength was considered, coating with ultra-fine slag and pretreatment with sodium hydroxide solution produced the most impressive results. Ultra-fine slag worked as fillers and generated calcium silicate compounds, which enhanced the microstructure of the Ru-GPC more than coating it with cement paste. Pretreatment of CRu particles, specifically coating with ultra-fine slag, improved the flexural strength, splitting strength, and modulus of elasticity (MOE) somewhat as well [141]. In terms of acid resistance, pretreatment with a sodium hydroxide solution was most successful, producing the maximum residual strength after 90-d of immersion in sulfuric and hydrochloric acids [141].

### 4.2. Mixing approaches

The AAS was prepared 24 h before blending in most Ru-GPC

experiments [96,99,124]. In terms of blending, dry ingredients such as A-S precursors, coarse aggregates, fine aggregates, and rubber particles were blended for 2–5 min first. After mixing for 2–5 min, the extra water and AAS were added to the dry materials. Admixtures were then gradually added and mixed for a further 1–2 min. Concrete was subsequently cast in the prepared molds, and samples were frequently compacted into two or three layers using a vibrating table to ensure dense samples. Fig. 8 illustrates this technique schematically. Numerous studies on Ru-GPC started with blending the A-S precursor with the AAS for 3–5 min, then add the natural aggregate and rubber particles, blending for another 5 min, casting, and compaction [103,126].

#### 4.3. Curing methods

The curing approaches for Ru-GPC samples are listed in Table 7: ambient curing, autoclave/steam curing, oven/heat curing, and water curing. Unlike PC-concrete, water curing is not commonly used with GP mixtures due to the possibility of free alkalis leaching through the pores of the concrete, which leads to the chemical instability of the GP mixture [147,148]. Curing samples at elevated temperatures improves strength growth, particularly for fly ash-based GPC [113]. Heat curing is a process that involves putting samples in an oven at temperatures ranging from 60 to 90 °C for 24–72 h, after which they are returned to ambient temperature until tested [118]. On the other side, steam curing entails putting samples in an autoclave for 7-d at a temperature of around 46 °C [102]. After that, the samples are removed and cured at room temperature until the test. According to Rajendran and Akasi [105], oven curing is one and a half times more effective than steam curing.

Luhar, Chaudhary and Dave [128] studied the influence of oven curing duration (24, 48, and 72 h) on the compressive strength of Ru-GPC samples, concluding that 48 h of curing was optimal. Moreover, the compressive strength of Ru-GPC rose with curing temperatures, although only slightly above 75 °C. As an option to heat curing, ambient curing is an appealing approach since it results in less concrete shrinkage, greater energy efficiency, and fewer surface cracks than heat curing [149,150]. Moreover, it was demonstrated that GGBFS-based alkali-activated concrete and rubberized alkali-activated concrete can

achieve high compressive strength under ambient curing conditions and do not need thermal curing [151,152].

## 5. Fresh and physical properties

### 5.1. Workability, flowability, and setting time

Concrete flow is reduced when CRu particles are used instead of natural aggregate [100,153,154]. For instance, when 20, 40, and 60% of fine aggregate were replaced with CR, the slump was reduced by 16%, 35%, and 52%, respectively, compared to the reference mixture [126]. Likewise, 30% CRu substitution for fine aggregate and coarse aggregate led to a 17.6% slump reduction as compared to the reference mixture (from 175 to 140 mm) [106]. This decrease in workability has been linked to the reduced relative density of CRu particles relative to natural aggregate, which results in less flow caused by self-weight [145]. Moreover, mechanically processed CRu particles have a larger overall surface area and rougher surfaces than natural aggregate particles, which demands the use of more water to overcome interparticle friction [1,155]. Due to the hydrophobic properties of CRu, they trap air in blending, increasing flow resistance and reducing workability [126].

Apart from the influence of CRu substitution on workability, the ratio of AAS to A-S precursor, the SS/SH ratio, and the molarity of sodium hydroxide also influence Ru-GPC flow, as shown in Fig. 9. Increasing the AAS to A-S precursor ratio is equivalent to increasing the mix's water content in PC-concrete and improving workability [156]. When it relates to sodium hydroxide content, higher molarity leads to a stiffer fresh mixture and, consequently, decreased workability [107]. A similar negative influence on workability is observed when the SS/SH ratio is increased, as the increased sodium hydroxide tends to increase the viscosity of the fresh mixture [107,157]. Preferring CRu particles with a sodium hydroxide solution decreases Ru-GPC workability since rougher CRu particles have improved flow resistance and adhesion properties [101].

When rubber particles are added to GPC, the initial and final setting times increase [111]; for example, the initial and final setting times of Ru-GPC mixtures containing 10% natural rubber latex were 85 and 135



Fig. 8. Mix design method for Ru-GPC.

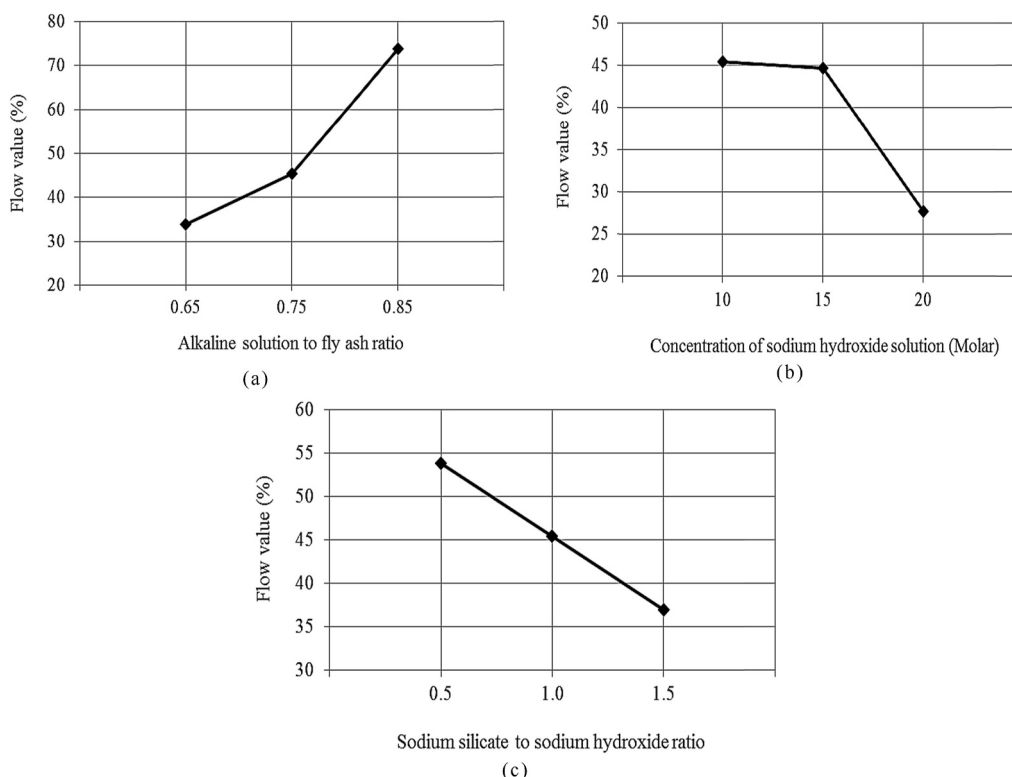


**Fig. 9.** Effect of (a) AAS to fly ash ratio, (b) concentration of sodium hydroxide solution, and (c) sodium silicate to sodium hydroxide ratio on the flowability of CRu geopolymer mortar [107].

min, respectively [111]. In comparison, the reference samples had an initial and final setting time of 62 and 106 min, respectively, demonstrating an increase due to the inclusion of rubber latex. This is partly because of the water contained within the pores of the CRu particles, which resulted in a modest increase in the total mixture's water content. Likewise, as shown in Fig. 10, introducing 2% rubber fibers to Ru-GPC mixtures can increase the initial and final setting times by 36% and 22%, respectively [142].

## 5.2. Water absorption and porosity

The water absorption and porosity of Ru-GPC samples are influenced by several parameters, such as the porosity of CRu particles, the volume

of entrapped air in the mixture, the alkaline liquid to solid binder ratio, and the characteristics of the CRu particles' interaction with the GP binder [158]. When CRu particles are added to GPC, the water absorption and porosity generally increase [123]. Wongsu, Sata, Nematollahi, Sanjayan and Chindaprasirt [107] found that 100% CRu substitution of fine aggregate increased the water absorption and porosity of rubberized geopolymer mortar mixtures by 5.7 and 1.5 times, respectively, compared to the reference mixture. Similarly, Dehdezi, Erdem and Blankson [125] indicated an increase in porosity from 23% in the control mixture without CRu substitution to 27.4% and 29.8% in Ru-GPC mixtures with 20% and 50% CRu substitution, respectively, by weight of fine aggregate. This happens as a result of increased CRu substitution, which results in more entrapped air in Ru-GPC, raising the total

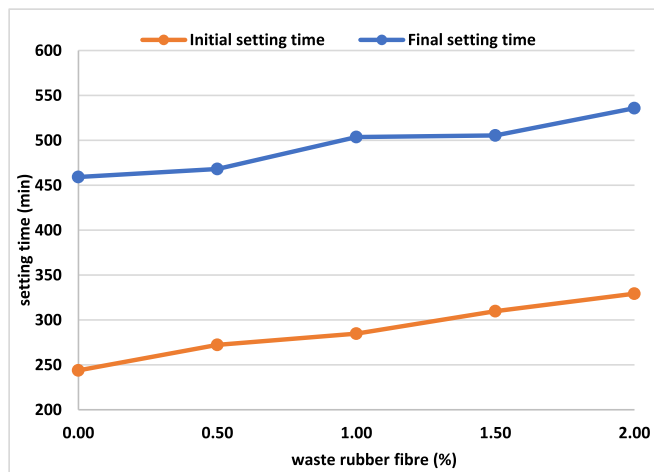


**Fig. 10.** Effect of waste rubber fiber on the initial and final setting times of low calcium-based GPC [142].

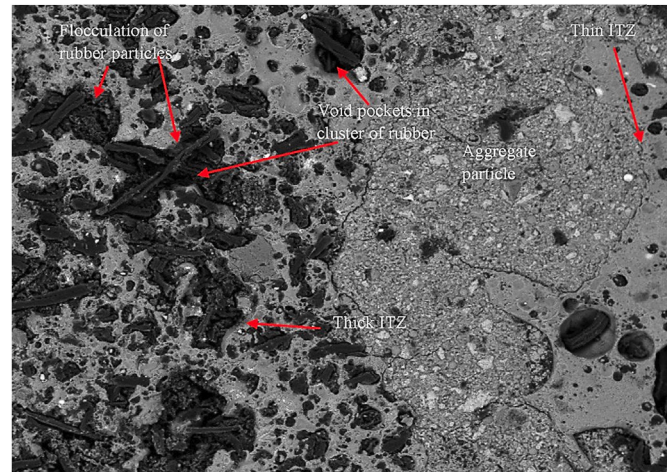


**Fig. 11.** SEM picture showing micro-scale features in rubberized concrete [125].

porosity, as shown in Fig. 11.

Moreover, a larger ratio of AAS to A-S precursor contributed to increased porosity in Ru-GPC mixtures, but higher curing temperatures and higher molarity of sodium hydroxide led to decreased porosity [98]. Additionally, the water absorption capacity of the Ru-GPC mixes increased when the curing temperature and SS/SH ratio rose [98]. Pretreatment of CRu particles with sodium hydroxide resulted in a small decrease in water absorption due to enhanced adhesion between the GP mixture and the CRu particles. Moreover, Fig. 12 presents the water absorption of Ru-GPC versus CRu substitution based on previous studies.

### 5.3. Density

The density of Ru-GPC samples decreased when the ratio of CRu to natural aggregate increased [99]. For example, Yahya, Abdullah, Ramli, Minciuna and Abd Razak [103] showed a drop in Ru-GPC density of 4.1% and 7.2%, respectively, when coarse aggregate was 10% and 20% were substituted with 5–10 mm CRu particles. In the same way, replacing 30% of both fine and coarse aggregate with CRu caused a 15.5% drop in density, from 2340 kg/m<sup>3</sup> to 1980 kg/m<sup>3</sup> [122].

Wongsa, Sata, Nematollahi, Sanjayan and Chindaprasirt [107] investigated the density of rubberized geopolymer mortar mixtures, including 100% CRu aggregate substitution, which was found to be between 1067 and 1275 kg/m<sup>3</sup>, or around 42% less dense than the control mix. This decrease in density associated with increased CRu substitution of natural aggregate can be related to the decreased relative density of CRu particles compared to natural aggregate, their larger internal pore capacity, and their tendency to entrap air in the mixture because of their toothed surfaces, as shown in Fig. 13 [124].

Rubberized geopolymer mortar mixtures had lower densities (1075–1950 kg/m<sup>3</sup>) than rubberized concrete mixtures (1299–2150 kg/m<sup>3</sup>) at the same CRu percentage replacement (25, 50, 75, and 100%) [140]. A-S precursors (GGBFS and fly ash) have lower specific gravity than PC. Moreover, increasing the ratio of AAS to A-S precursor led to a slight decrease in density in Ru-GPC mixtures [107]. Conversely, increasing the molarity of sodium hydroxide results in an increase in Ru-GPC density [107]. Moreover, Fig. 14 presents the density of Ru-GPC versus CRu substitution based on previous studies. The figure indicates that the increase in the percentage of replacing the rubber aggregate increases the decrease in the density. This behavior is generally related, as previously mentioned, to the lower relative density of CRu particles compared to natural aggregates, their ability to have larger internal pores, and their tendency to trap air in the mixture due to their serrated surfaces.

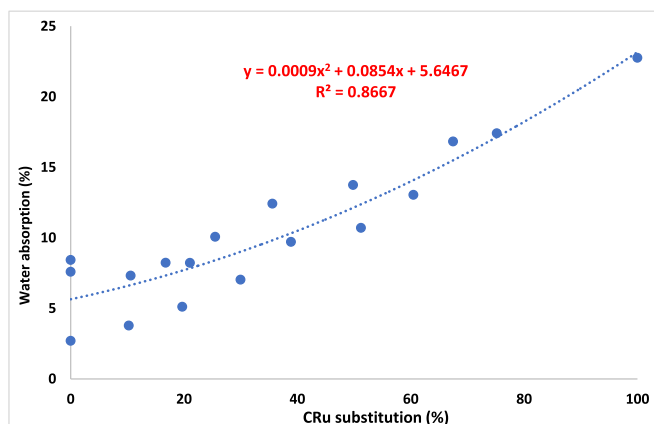


Fig. 12. The water absorption of Ru-GPC versus CRu substitution [106, 107, 159–161].

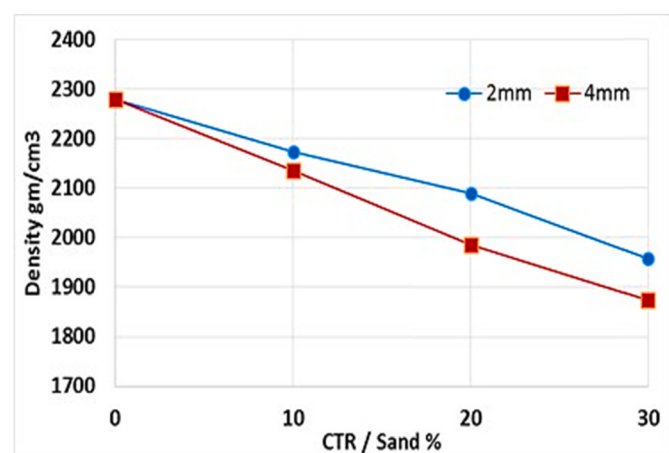


Fig. 13. The 28-d density at various chopped tire rubber (CTR)/sand ratios [124].

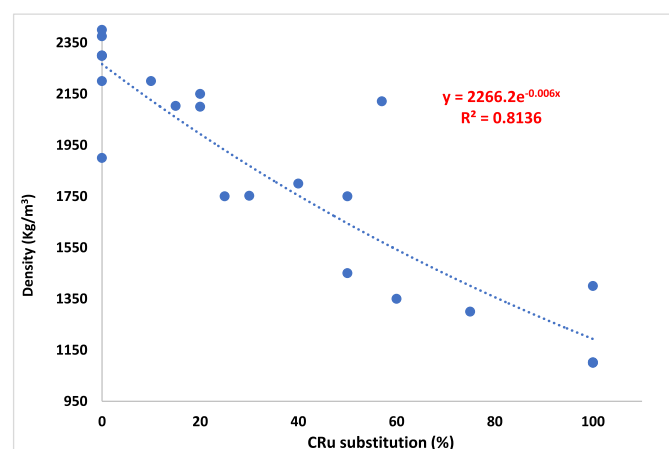


Fig. 14. The density of Ru-GPC versus CRu substitution [106, 107, 159, 160, 162].

## 6. Mechanical properties

### 6.1. Compressive strength

Increased CRu particle content in Ru-GPC leads to decreased compressive strength, irrespective of the A-S precursor type, curing conditions used, or AAS used [102, 104, 118]. Azmi, Abdullah, Ghazali, Sandu and Hussin [104] found a compressive strength decrease of up to 60% for fly ash-based rubberized geopolymer mortar when 15% CRu was replaced by a volume of fine aggregate. As shown in Fig. 15, Zhong, Poon, Chen and Zhang [95] observed that when 15% CRu was substituted for fine aggregate, the 28-d compressive strength decreased by 36.9%. Wongsa, Sata, Nematollahi, Sanjayan and Chindaprasirt [107] showed that when fine aggregate and coarse aggregate were completely replaced with CR, the 28-d compressive strength decreased by about 93% and varied between 2 and 3.3 MPa, keeping within the required strength scope for lightweight moderate strength concrete (2–14 MPa) [163].

The reasons for the decline in compressive strength for Ru-GPC with increased CRu replacement are similar to those for rubberized concrete and can be summarized in the following: (a) the hydrophobic property of CRu results in a poor bond with the GP mixture, leads to the development of a weak ITZ; (ii) CRu particles have a lower MOE than the surrounding GP mixture, leads to high-stress intensity within them and later development of micro-cracks around them, leads to compressive

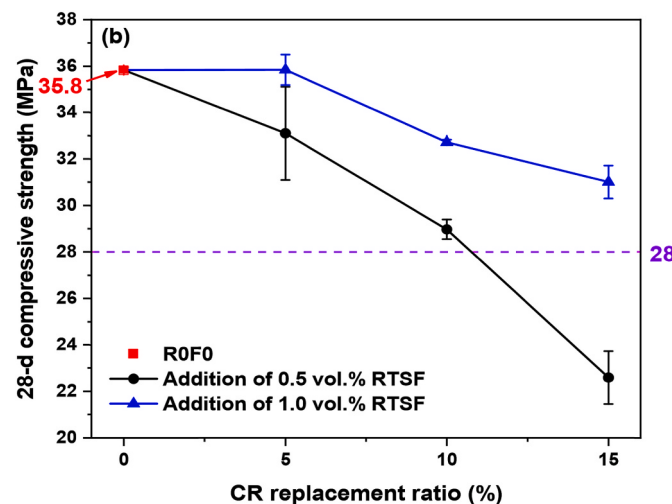


Fig. 15. Effects of CRu and recycled tire steel fiber (RTSF) on compressive strength [95].

strength decline; and (iii) the existence of CRu particles in Ru-GPC, and (iv) the jagged and rough surface of the CRu particles increases the number of entrapped air bubbles in the Ru-GPC mix, increasing the overall porosity and lowering compressive strength.

Apart from the rubber replacement ratio, the compressive strength of Ru-GPC is dependent on several influences, such as the following: (a) the A-S precursor, (b) the alkaline solution, (c) the AAS to A-S precursor ratio, (d) the aggregate size, (e) the CRu particle size, and (f) the curing conditions. The amount of calcium oxide in the A-S precursor significantly affects compressive strength. For instance, Park, Abolmaali, Kim and Ghahremannejad [102] showed that when several fly ash-based Ru-GPC mixtures were compared, the mixture with a higher calcium oxide concentration in the fly ash showed the highest compressive strength, as shown in Fig. 16. Furthermore, for the same kind of fly ash, larger particle sizes (50–200  $\mu\text{m}$ ) led to a greater drop in compressive strength with increased CRu addition than smaller particle sizes (1–60  $\mu\text{m}$ ) [102]. Moreover, Dong, Elchalakani, Karrech and Yang [106] reported that increasing the proportion of GGBFS in the fly ash-based Ru-GPC mixture from 20% to 40% of the overall binder volume led to a 33% increase in the 28-d compressive strength, which was directly proportional to the higher calcium oxide level in GGBFS.

Park, Abolmaali, Kim and Ghahremannejad [102] demonstrated that for the same sort of fly ash and CRu substitution ratio, the mixture with

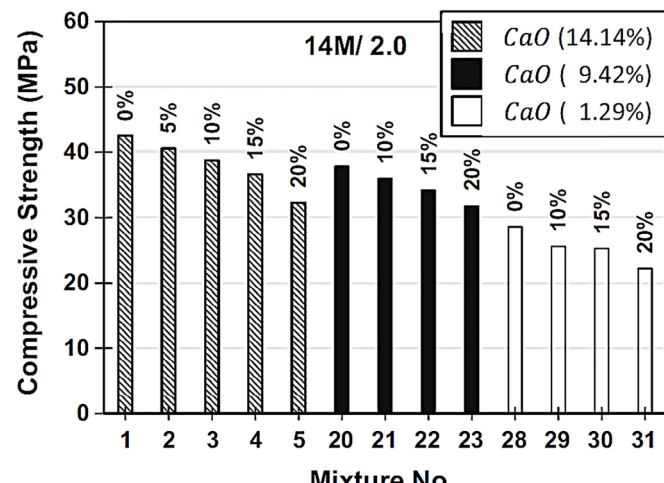


Fig. 16. Comparison of compressive strength concerning the type of fly ash [102].

14 molarity sodium hydroxide doses obtained a greater 7-d compressive strength than the mix with 8 molarity, as shown in Fig. 17. Moreover, Luhar, Chaudhary and Dave [128] showed a continuous increase in compressive strength as the molarity of sodium hydroxide was raised from 10 to 14 molarity. Wongsa, Sata, Nematollahi, Sanjayan and Chindaprasirt [107] found a 9.7% increase in compressive strength when the molarity of the sodium hydroxide solution was raised from 10 to 15 molarity, but a 13.2% decrease in compressive strength when the molarity was increased further to 20 molarity, as shown in Fig. 18. Similarly, with GPC, the optimal sodium hydroxide molarity was 14 molarity [164]. This shows that the ideal sodium hydroxide molarity for increasing compressive strength is between 14 and 15 molarity.

Moreover, previous research has demonstrated that the ratio of SS/SH affects compressive strength [102]. For example, Park, Abolmaali, Kim and Ghahremannejad [102] observed an increase in compressive strength of up to 40.7% when the SS/SH ratio was adjusted from 0.5 to 2, as shown in Fig. 19. Increased sodium hydroxide content in the mixture leads to increased dissolution, which enhances the microstructure. Nevertheless, it was shown that raising the SS/SH ratio over 2 had an adverse effect on compressive strength. According to Luhar, Chaudhary and Dave [128], raising the SS/SH ratio from 1.5 to 2 increased compressive strength, but increasing it from 2 to 2.5 decreased strength. The results indicate that the optimal SS/SH ratio is 2.

Compressive strength is decreased by increasing the AAS to A-S precursor ratio from 0.65 to 0.85 [107]. Meanwhile, increasing the AAS to fly ash ratio from 0.3 to 0.35 increased compressive strength, but raising it further to 0.4 decreased compressive strength [129].

Aslani, Deghani and Asif [98] conducted trial tests to identify the optimal Ru-GPC mix design, varying the ratio of AAS to A-S precursor from 0.4 to 0.6 and settling on 0.4 as the optimal value. This indicates that the optimal AAS to A-S precursor ratio is between 0.35 and 0.4 to produce a high strength Ru-GPC.

In addition to the above, it has been demonstrated that utilizing bigger coarse aggregate (16 mm) in Ru-GPC mixes results in better compressive strength than mixes using smaller coarse aggregate (9.5 mm) [102], which may be because of the increased interlocking among the larger aggregates [165]. The compressive strength of Ru-GPC mixtures can also be affected by the size of CRu particles. Using bigger CRu particles (5–10 mm) resulted in an 8.2–9% drop in compressive strength when compared to Ru-GPC mixes with smaller CRu particles (2–5 mm) [98]. Likewise, Ru-GPC mixes containing 2 mm CRu particles had a compressive strength of 8.3–15.9% more than mixes containing 4 mm CRu particles while keeping the same CRu replacement percentage of fine aggregate [124]. According to previous research, Figs. 20 and 21 show the normalized compressive strength versus CRu substitution and the relationship between the compressive strength and water absorption of Ru-GPC.

## 6.2. Splitting tensile strength

Aslani, Deghani and Asif [98] found a decrease in the 28-d splitting tensile strength, as shown in Fig. 22, from 2.26 MPa for reference samples to 1.84 MPa (18.6% lessening) and 1.82 MPa (19.5% lessening) for 10% and 20% CRu substitution of fine aggregate, respectively. Aly, El-Feky, Kohail and Nasr [116] reported a 35.5% reduction in splitting tensile strength with a 30% CRu substitute of natural aggregate, while Dong, Elchalakani, Karrech and Yang [106] reported a similar decrease in splitting tensile strength from 3.5 MPa for reference samples to 1.2 MPa (65% decrease) and 0.7 MPa (80% decrease) with 15% and 30% CRu substitute of coarse aggregate, respectively. Reduced adhesion among CRu particles and the surrounding GP mixture due to rubber's hydrophobic characteristics and the development of a weaker interfacial transition zone around the CRu particles are the causes of this decrease.

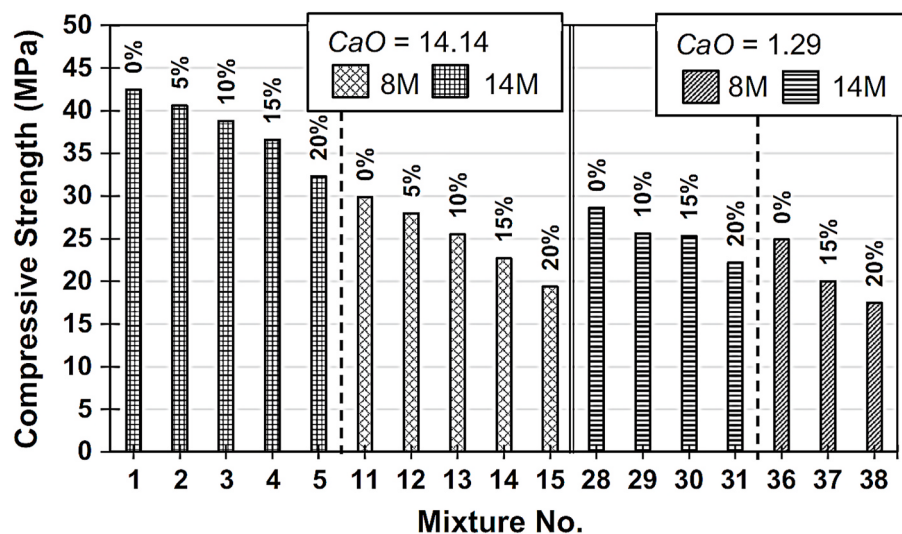


Fig. 17. Comparison of compressive strength concerning the type of molarity [102].

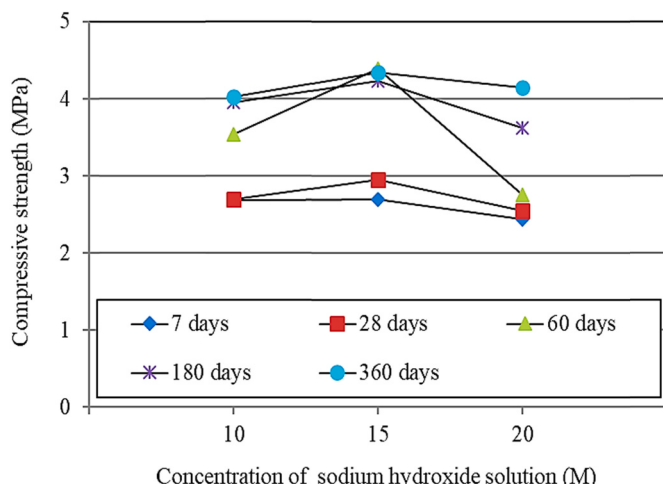


Fig. 18. Effect of sodium hydroxide concentration on compressive strength [107].

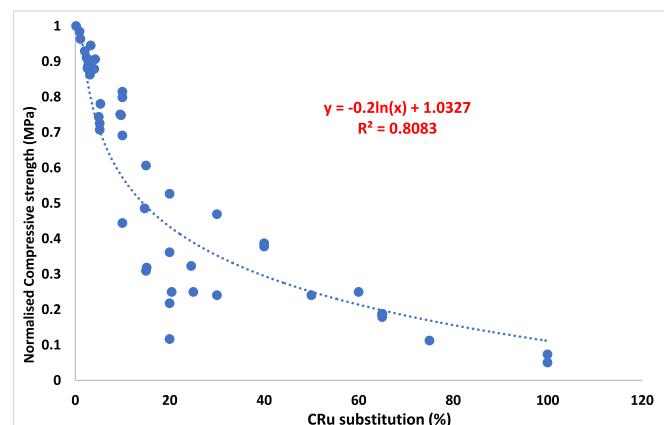


Fig. 20. The compressive strength of Ru-GPC versus CRu substitution [102, 106, 107, 121, 122, 159, 161, 166–169].

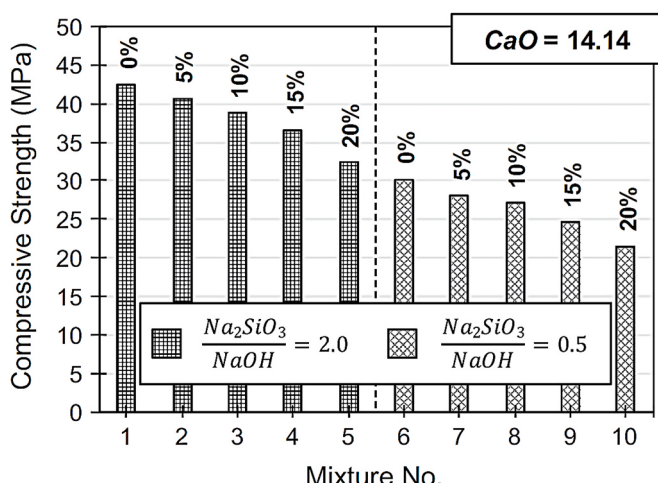


Fig. 19. Comparison of compressive strength concerning the ratio of alkaline solutions [102].

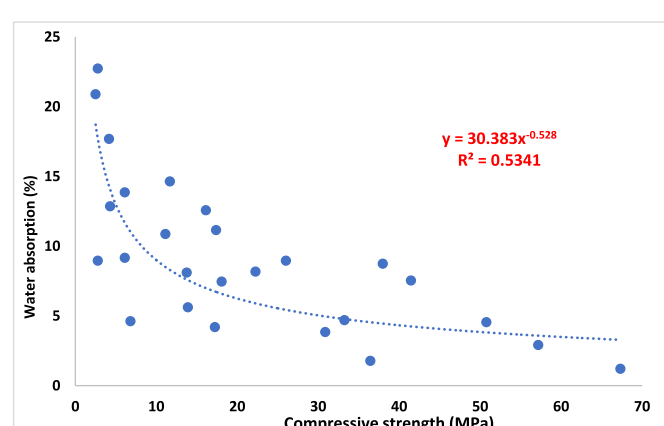
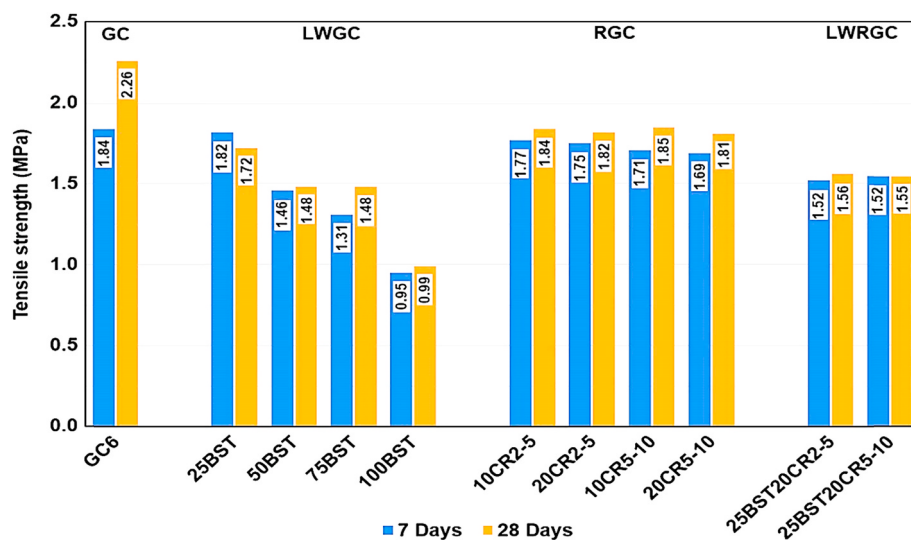


Fig. 21. The relationship between compressive strength and water absorption of Ru-GPC [104, 106, 107, 126, 140].

### 6.3. Flexural strength

The flexural strength of Ru-GPC decreased proportionately with increasing CRu substitution, similar to compressive strength [100]. Aly, El-Feky, Kohail and Nasr [116] indicated a decrease in flexural strength



**Fig. 22.** Tensile strength of developed geopolymer concrete (GC), lightweight geopolymer concrete (LWGC), rubberized geopolymer concrete (RGC), and light-weight rubberized geopolymer concrete (LWRGC) mixes at 7 and 28-d [98].

of up to 20% with 10% CRu substitution of fine aggregate and coarse aggregate and a 30% decrease in flexural strength with 20% CRu substitution. Rajaei, Shoaei, Shariati, Ameri, Musaei, Behforouz and de Brito [126] indicated a reduction in flexural strength of up to 74% when fine aggregate was replaced with 60% CR, as shown in Fig. 23. Meanwhile, Zaetang, Wongsa, Chindaprasirt and Sata [140] reported flexural strength decreases of 61.4%–77.3% when fine aggregate and coarse aggregate were replaced with 50% and 100% CR, respectively, compared to reference samples. The cause of the decrease in flexural strength is mostly due to the low adherence of CRu particles to the matrix.

#### 6.4. Modulus of elasticity (MOE)

The MOE of Ru-GPC samples decreased as more CRu was substituted for natural aggregate [121]. The 28-d MOE decreased from 30 GPa for reference samples to 18.2 GPa (by 39%) and 7.8 GPa (by 74%), respectively, for samples with 15% and 30% CRu substitution of coarse aggregate [106]. Similar findings were noted by Rajaei, Shoaei, Shariati, Ameri, Musaei, Behforouz and de Brito [126], who detected decreases in MOE of around 29%, 66%, and 81% for samples with 20%, 40%, and 60% CRu substitution of fine aggregate, respectively. Luhar, Chaudhary and Luhar [121] also found a drop in MOE of up to 36.3% when rubber

fibers were added to the GP mixture to substitute up to 30% by weight of fine aggregate, as shown in Fig. 24. This decrease in MOE with increased CRu substitution is owing to the CRu particles' softness and deformability. CRu can be used instead of natural aggregate to make concrete that is more flexible and has a lower MOE [170].

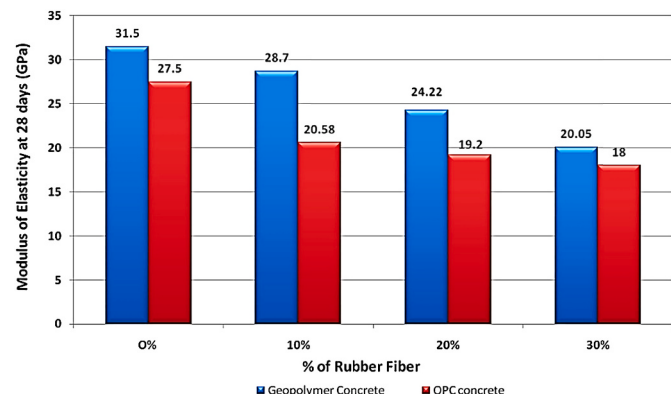


**Fig. 24.** Modulus of elasticity of PC and GPC [121].

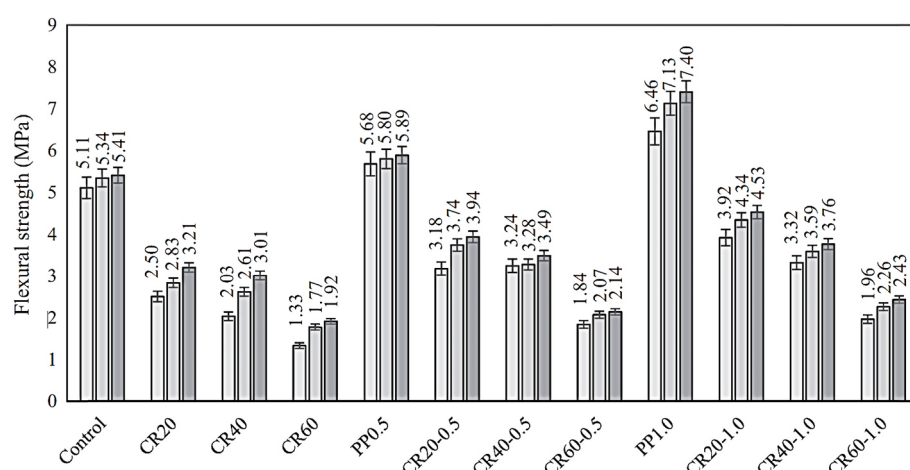


**Fig. 23.** Flexural strength of mixes at various ages [126].

### 6.5. Stress-strain curve

To effectively assess the effect of CRu aggregates on the GP paste's flexural response and deflection curve under compression, the sample's stress-strain curves should be analyzed. Fig. 25 from the study of Hamidi, Valizadeh and Aslani [171] depicts the stress-strain curves for ambient-cured control GPC, Ru-GPC, and Lightweight GPC depending on 28-d findings. According to the authors, when the normal stress-strain curve for normal concrete under compression is considered, the ascending branch of the stress-strain curve consists of two distinct areas: the initial upward linear area and the non-linear strain-hardening zone. The concrete will exhibit elastic behavior under compression with no cracks inside the cement paste until the load approaches the binder's cracking limit. The steeper the linear section, the greater the sample's strength, which implies that the concrete exhibits less deflection before cracking development. In the non-linear strain-hardening zone, the concrete undergoes irreversible plastic deformation because of the formation of several micro-cracks within the paste of cement at the interaction among the paste and the aggregates, until it reaches the yield point, which is the maximum stress that a concrete sample can withstand in compression [172,173]. Up to about 40% of the peak load, the initial linear elastic area exists [174], and the MOE of the concrete sample can be calculated as the proportion of the stress equivalent to 40% of the yield strength and its associated strain [175,176]. The sloped branch of the stress-strain curve contains the plastic strain-softening area, in which a high number of micro-cracks develop in the concrete, and these localized micro-cracks define the concrete's ductility [173, 174]. The GPC stress-strain profile is comparable to that of normal concrete.

Zhong, Poon, Chen and Zhang [95] investigated the deflection behavior of an alkali-activated binder reinforced with recycled steel fibers, including CRu aggregates instead of fine aggregates, as shown in Fig. 26. They discovered that adding more than 10% CRu aggregates decreased the elastic effectiveness of the recycled steel fiber-reinforced alkali-activated binder comprising CRu aggregates but did not affect the strain-hardening behavior of the steel fiber-reinforced alkali-activated binder, whereas raising the steel fiber dosage prolonged the deflection-hardening phase.

In a previous study by Hamidi, Valizadeh and Aslani [171], the authors summarized their findings by stating that the stress-strain curves of the Ru-GPC also revealed that 10% CRu aggregates might be the optimal rubber aggregate concentration within the GPC paste to ensure the

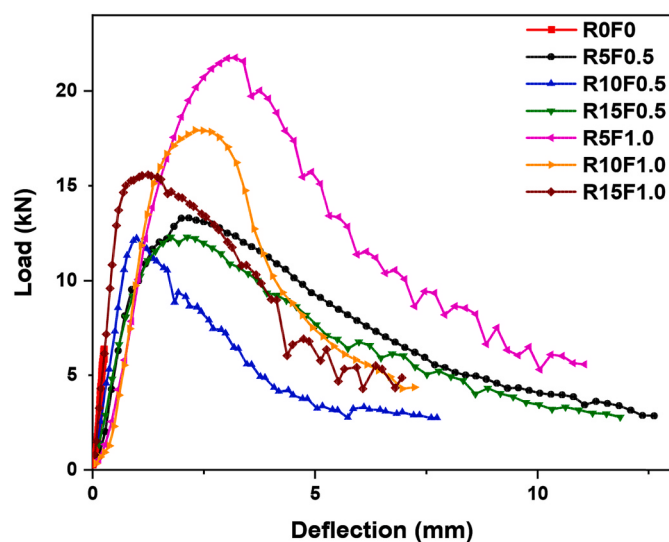


Fig. 26. Load-deflection curve under four-point bending [95].

desired load-bearing capacity and delay the occurrence of cracks. This may be due to the more compacted microstructure of the Ru-GPC comprising 10% CRu aggregates, the development of the A-S gel, and, consequently, the interfacial transition zone among the paste and the rubber aggregates over the 28-d curing process. When the rubber aggregates volume exceeds 10%, the CRu aggregates' filling capacity decreases, behaving as voids inside the GPC paste. At less than 10%, CRu aggregates are inadequate to form a thick microstructure and, consequently, impair the uniformity of the paste at low binder concentrations.

## 7. Dynamic properties

### 7.1. Strain rate effects

Pham, Liu, Tran, Pang, Shi, Chen, Hao and Tran [122] exposed  $\varphi 100 \times 50$  mm Ru-GPC samples to split Hopkinson pressure bar tests at strain rates of 50, 70, 90, and 1301/s, as shown in Fig. 27. The split Hopkinson pressure bar test is commonly applied to characterize the dynamic characteristics of concrete samples exposed to moderate to high strain levels and to measure their dynamic increase factor [177, 178]. The results indicated that when subjected to high strain levels, Ru-GPC samples stayed intact, but those without CRu entirely collapsed. The stress-strain curves of samples are similarly altered by the CRu partial substitute of natural aggregate, with samples containing CRu having a flatter sloped stress-strain branch following the peak load, denoting increased ductility with increasing CRu addition [122]. It has been demonstrated that when CRu substitution increases, the dynamic compressive strength of Ru-GPC mixtures decreases [122]. The reference samples demonstrated that with 0% CRu substitution, they had a greater dynamic compressive strength than the samples with 15% and 30% CRu substitution of fine aggregate and coarse aggregate.

On the other hand, the dynamic increase factor was higher in samples with a higher rate of CRu substitution. For example, mixtures containing 30% CRu showed a dynamic increase factor of 1.37–3.4 when strain rates varied between 50 and 1301/s [122]. In comparison, at the same strain rates, reference normal samples showed a dynamic increase factor of 1.04 and 1.87 [122]. This increase in dynamic increase factor results from the increased deformability of CRu and their ability to inhibit crack development [116].

### 7.2. Impact resistance properties

Aly, El-Feky, Kohail and Nasr [116] conducted a drop weight test

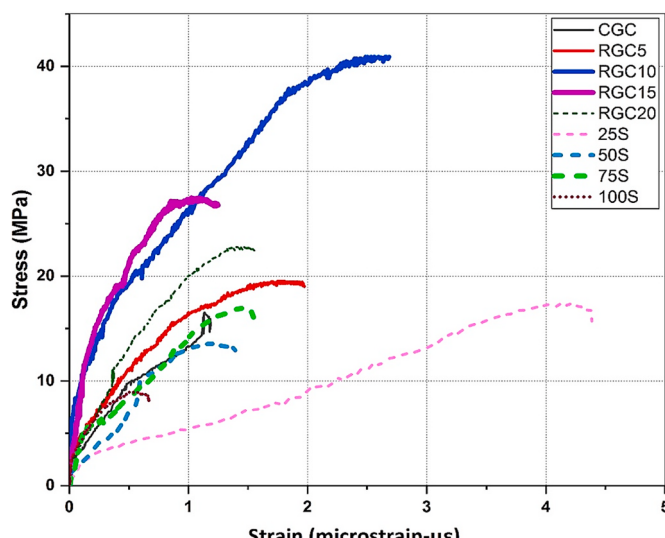
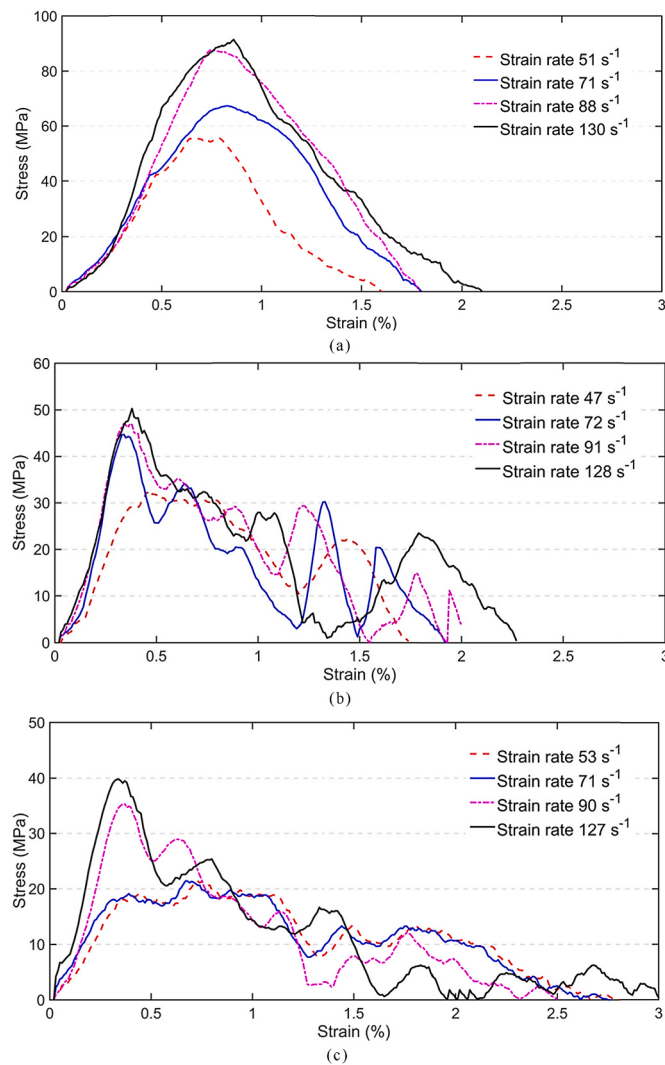


Fig. 25. Stress-strain curves for Ru-GPC and Lightweight GPC under compression [171].



**Fig. 27.** Stress-strain diagrams of (a) 0%, (b) 15%, and (c) 30% Ru-GPC at different strain rates [122].

using cylindrical rubberized alkali-activated concrete discs ( $\phi 150 \times 65$  mm) following AC-544 [179]. The test involved lowering a 4.5 kg steel ball from a predetermined height of 450 mm. The number of strikes required to initiate and finish cracks in the concrete discs was measured. The results showed that when the CRu ratio was increased, more strikes caused both an initial crack and a final crack, which meant that the material's impact resistance went up as well.

Dehdezi, Erdem and Blankson [125] conducted a drop weight test on Ru-GPC samples using the Erdem, Dawson and Thom [180] method, in which a cylindrical steel ball weighing 5 kg was felled from a preset height of 1 m. Initial cracks developed at 3, 5, and 7 strikes for GPC mixtures containing 0%, 20%, and 50% CRu of fine aggregate, respectively. The final strikes were 4, 17, and 38, with failure impact energies of 250 kN mm, 900 kN mm, and 1900 kN mm for each mixture. Increased CRu content in rubberized alkali-activated concrete improves impact resistance, as shown in Fig. 28, because of the increased deformability and reduced stiffness of CRu particles, which improve energy absorption and flexibility [116]. Unlike GP paste and natural aggregate, rubber particles can assist in preventing crack development and boost impact strength when subjected to impact loading [180]. Rubberized alkali-activated concrete discs also had a more ductile failure, as shown by the production of several cracks, while control discs without CRu addition failed with a single massive crack, frequently splitting the discs in half.

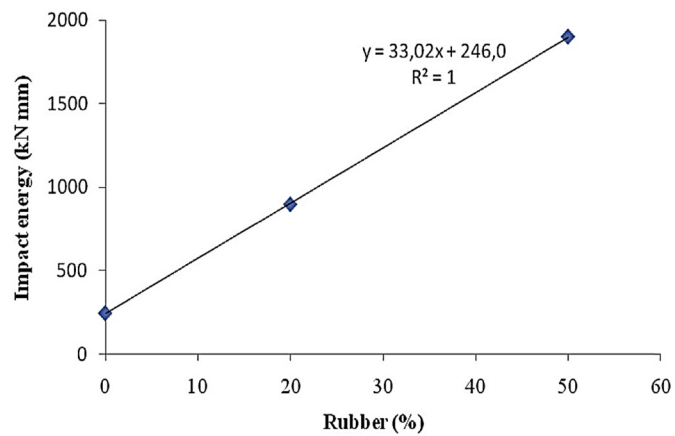


**Fig. 28.** Relationship between impact energy of concrete and rubber content [180].

## 8. Durability properties

According to Rajaei, Shoaei, Shariati, Ameri, Musaei, Behforouz and de Brito [126], the drying shrinkage of Ru-GPC samples with a 20%, 40%, and 60% CRu substitution for fine aggregate rose by 18%, 34%, and 57%, respectively, as compared to the reference sample. This increase is attributable to the decreased stiffness and increased flexibility of CRu particles, which provide little resistance to paste shrinkage when the mixture dries [181]. Moreover, the limited adhesion between the surrounding GP mixture and the CRu particles limits shrinking to a minimum owing to reduced internal friction.

Moghaddam, Madandoust, Jamshidi and Nikbin [120] evaluated the resistance to sulfuric conditions by immersing Ru-GPC samples with a 10% CRu substitution of fine aggregate in a 5% sulfuric acid solution with a pH of 1 for up to 90-d. As shown in Fig. 29, some of the fly ash in the Ru-GPC samples was substituted by PC (up to 20%), and the results revealed that mixtures with a larger PC substitution of fly ash had more mass loss. For example, with 0%, 10%, and 20% PC substitution, mass decreased by 4.7%, 5.4%, and 8.1%, respectively. Furthermore,

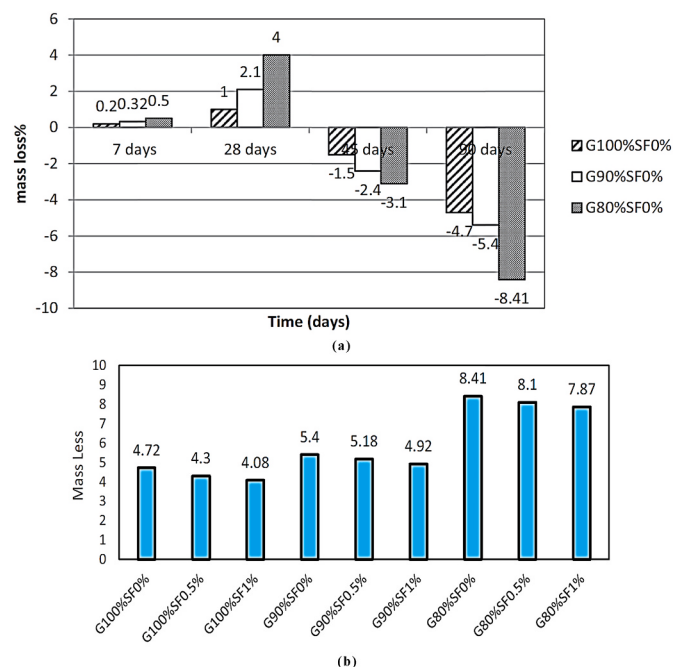


**Fig. 29.** Mass Less of GPC samples exposed to sulfuric acid: (a) 7 to 90-d, (b) after 90-d [120].

compressive strength results show that Ru-GPC samples with more PC substitution were more sensitive to sulfuric acid exposure and lost more strength when they were exposed to sulfuric acid.

Luhar, Chaudhary and Luhar [121] observed that more rubber substitution of fine aggregate increased the abrasion resistance of Ru-GPC samples after 28-d, as evaluated by wear depth, as shown in Fig. 30. For example, with 0% and 30% rubber fiber substitution of fine aggregate, the depth of wear was 1.28 mm and 0.8 mm, respectively, after 28-d. This increase in abrasion resistance may be partial because rubber particles elongate further than the smooth surface and act as brushes when exposed to abrasive forces, reducing the effect of the abrasive powder on the surface.

## 9. Chemical attacks

### 9.1. Resistance to sulfuric acid and hydrochloric acid attack

Pham, Lim and Malekzadeh [141] investigated the impact of replacing fine aggregates with CRu on the characteristics of GPC. Natural fine aggregates were partially substituted with CRu at a volumetric ratio of 10%, 20%, and 30%. The impact of pretreatment of CRu with water, sodium hydroxide, cement paste, and ultra-fine slag on the strength of GPC was investigated. The GPC mixtures were produced using 8 molarity sodium hydroxide and then heated to 60 °C for curing. Moreover, the durability characteristics of the material, such as acid attack resistance, were investigated experimentally. According to the authors, samples subjected to sulfuric acid and hydrochloric acid demonstrated similar declines in compressive strength. Yet, the highest strength was seen when sodium hydroxide-treated and ultra-fine slag-treated CRu were used. This is because the roughness of the surface caused by sodium hydroxide mechanically etching led to more matrix coating on the CRu surface, which led to better adhesion for the CR.

Moreover, sodium hydroxide functioned as a duty cleanser, assisting in removing dirt, grease, and other impurities from the CRu surface, leading to enhanced adhesion among CRu and other GPC ingredients. On the other side, ultra-fine slag, a pozzolana, functions as a filler material and fills the pores in GPC, leading to a denser matrix structure. The other main reason was to fix Ca(OH)<sub>2</sub>, the most sensitive product in an acidic environment. Previous research has indicated that the use of pozzolanic materials can aid in the prevention of aggressive chemicals, such as acids, from penetrating concrete [182]. Lee, Moon and Swamy [183] studied the sulfate attack resistance of concrete using silica fume and discovered that the inclusion of silica fume, a pozzolanic material comparable to ultra-fine slag, increased the sulfate resistance. The effect of sodium hydroxide pretreatment on the hydrophobicity of CRu particles was considerable; the contact angle was reduced [184], leading to a thinner water film forming on the CRu surface. More functional groups were produced due to sodium hydroxide degradation of the rubber chains, which resulted in the highly polar CRu surface. Increased O–H

groups increased the wettability of the CRu surface. Pretreatment decreased porosity at the interfacial transition zone [184], improving bonding between CRu and other GPC constituents and increasing GPC's strength. Numerous insoluble elements, such as zinc oxide, were transformed into water-soluble sodium ions that were easily removed; hence, sodium hydroxide improved the surface characteristics of CRu [185].

In the previous study by Pham, Lim and Malekzadeh [141], the authors summarized their findings by stating that GPC was susceptible to hydrochloric acid or sulfuric acid attack, with a maximum strength drop of 23.4% for the reference GPC. GPC containing CRu was more susceptible to acid attacks. When batch B3 was exposed to hydrochloric acid and sulfuric acid, it lost a small amount of its compressive strength. This loss was 7–18% and 10–22%, respectively.

## 10. Microstructures

Lazorenko, Kasprzhitskii and Mischinenko [161] investigated the influence of several physical and chemical pretreatments of CRu with H<sub>2</sub>SO<sub>4</sub>, NaOH, KMnO<sub>4</sub>, and (CH<sub>3</sub>)<sub>2</sub>CO solutions, and also ultraviolet (UV) light, on the mechanical properties and microstructure of rubberized fly ash-based GP composites. According to the authors, microstructure investigation of GP composite shattered surfaces using 3D laser confocal imaging, as shown in Fig. 31, confirms the findings of mechanical testing, suggesting a high adherence of CRu particles treated with KMnO<sub>4</sub> to the GP. The rubber particles are spread very equally throughout the GP matrix, as shown in Fig. 31-a. The fractured surfaces of all samples reveal a typical fly ash-based GP microstructure consisting of geopolymers products, trapped air pores, and tiny spaces from unreacted fly ash particles, consistent with earlier research [186–189]. On open rubber surfaces of GP/CR-PP, there are substantial changes in the ratio of residual geopolymers products, as shown in Fig. 31-g, compared to other composites, as shown in Fig. 31-(b–f). The GP binder strongly covers and bonds the potassium permanganate-treated CRu particles. It strongly covers and bonds the potassium permanganate-treated CRu particles, resulting in a continuous gel mass. There are no faults or delamination identified in the interfacial transition zone. This demonstrates the interplay between CR-PP and GP stages in forming structures. On the other hand, the surface of the rubber particles on the fractured surfaces of the remaining samples is relatively clean, and delamination and cavities are shown in certain parts of the contact zone among the GP and the filler, which refers to a lack of adhesion.

Moreover, Valente, Sambucci, Chougan and Ghaffar [160] investigated the microstructures of rubberized samples created by altering the binder, the sand rubber substitution ratio (0%, 50%, and 100%), and the rubber particle size (1–3 mm rubber granules and 0–1 mm rubber fine aggregate). The authors report that (i) microstructural evaluation reveals a significant variation in the interfacial adhesion of ground tire rubber aggregates with the two-binder composite, as shown in Fig. 32. Enhanced ground tire rubber-matrix compatibility was noted in GP mixtures as a result of the synergistic effect of sodium hydroxide and silica fume on the instinct chemical and physical activation of rubber, resulting in more ductile behavior under pending; (ii) the permeability and porosity rate of the mixtures were impacted by various microstructural properties of the rubber-interfacial matrix bond. Although the addition of ground tire rubber increased the permeable porosity and water absorption values in both matrices slightly, the GP formulations had lower values than their PC counterparts. Moreover, the decreased water content and self-compacting nature of the alkali-activated material formulations can reduce the incidence of permeable porosity in the hardened specimens.

In the previous study by Lazorenko, Kasprzhitskii and Mischinenko [161], the obtained parameters are consistent with the findings of water adsorption investigations and the chemical and morphological properties of CRu. This verifies the hypothesis that the chemical composition of the CRu surface and the strength of its contact with the GP have a

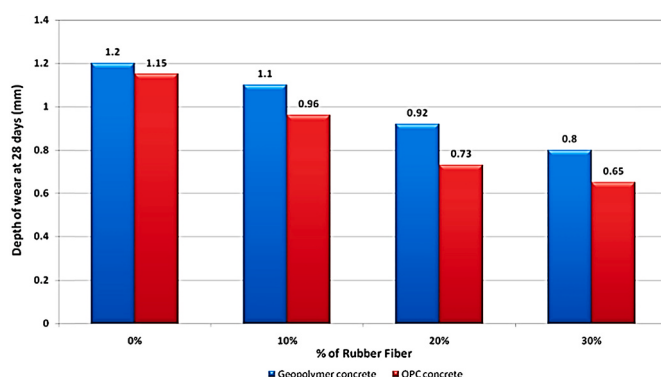
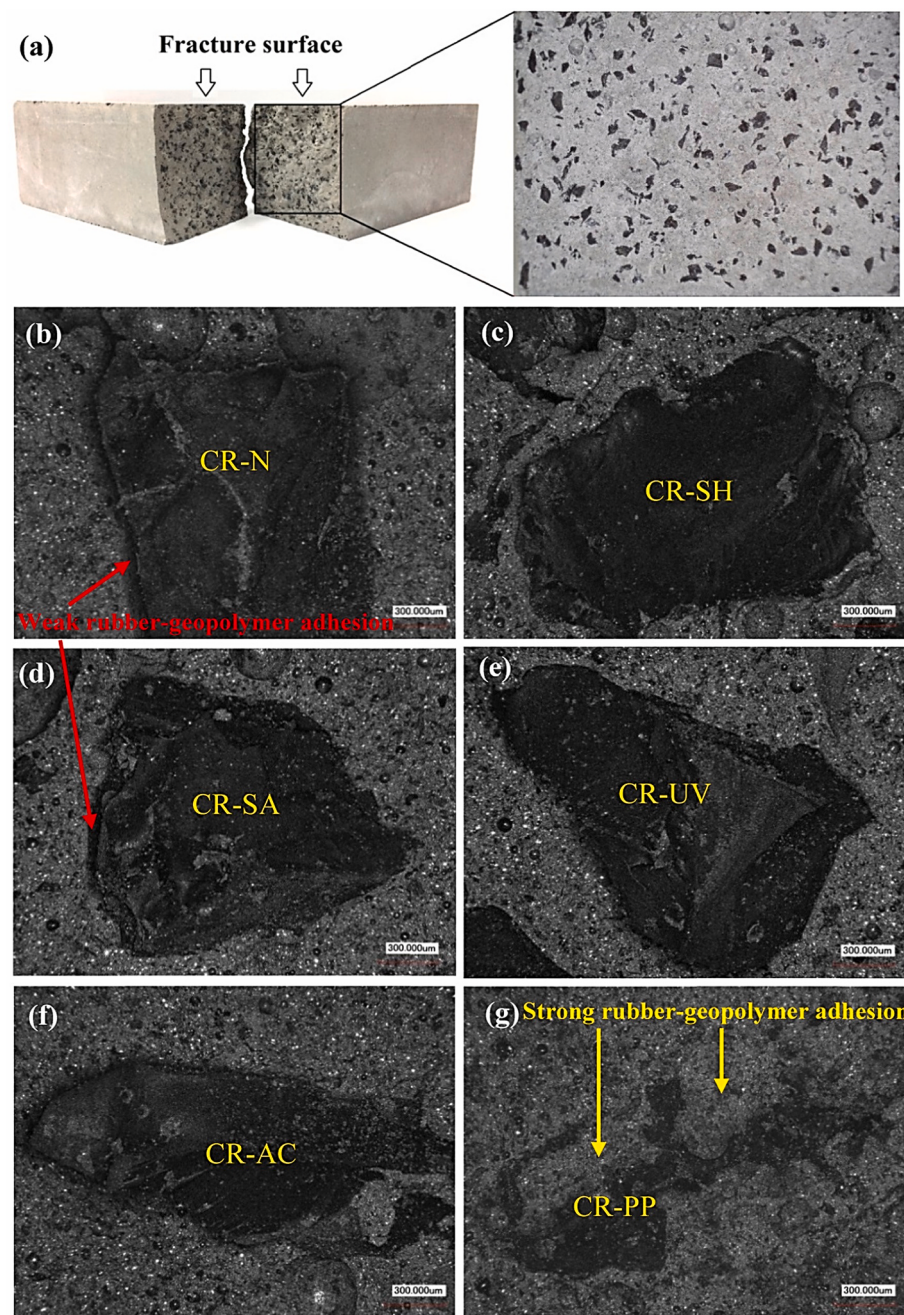


Fig. 30. Depth of wear for PC and GPC [121].



**Fig. 31.** (a) Photograph of the Ru-GPC after flexural tests (28-d) and the 3D laser confocal images of geopolymer composite fractured surfaces for the different CRu types: (b) native; (c) NaOH treated; (d)  $\text{H}_2\text{SO}_4$  treated; (e) UV treated; (f)  $(\text{CH}_3)_2\text{CO}$  treated; (g)  $\text{KMnO}_4$  treated [161].

significant effect on the strength of the composites investigated. The most polar (hydrophilic) groups on the surface of CR-PP particles establish strong hydrogen intermolecular interactions, as shown in Fig. 33, with oxygen sodium A-S hydrate ( $\text{N}-\text{A}-\text{S}-\text{H}$ ) gel and other geopolymers products coexisting with it [190,191]. These bonds are responsible for the strong adherence of rubber treated with  $\text{KMnO}_4$  to the GP binder, which reaches or surpasses the matrix's cohesive strength, favorably affecting the composite's strength properties. This is in line with findings from other researchers who looked at a wide range of dispersed and fibrous fillers [187,192,193]. They found that filler surface hydroxyl groups had a positive effect on the mechanical properties of GP composites.

## 11. Insulation properties

### 11.1. Thermal conductivity

The thermal conductivity of concrete is governed by various parameters, such as the type of aggregate used, the amount of air in the mixture, and the density [107]. According to Aslani, Deghani and Asif [98], the thermal conductivity of rubberized geopolymer mortar samples with a 100% CRu substitution of fine aggregate was, on average 79% lower than the nonrubberized reference sample. Zaetang, Wongsa, Chindaprasirt and Sata [140] found comparable results with rubberized geopolymer mortar samples, where the thermal conductivity was 1.07 W/mK for the reference sample and 0.19 W/mK for the sample with 100% CRu substitution of natural aggregate, showing a drop of up to 82% in thermal conductivity. This reduced thermal conductivity is

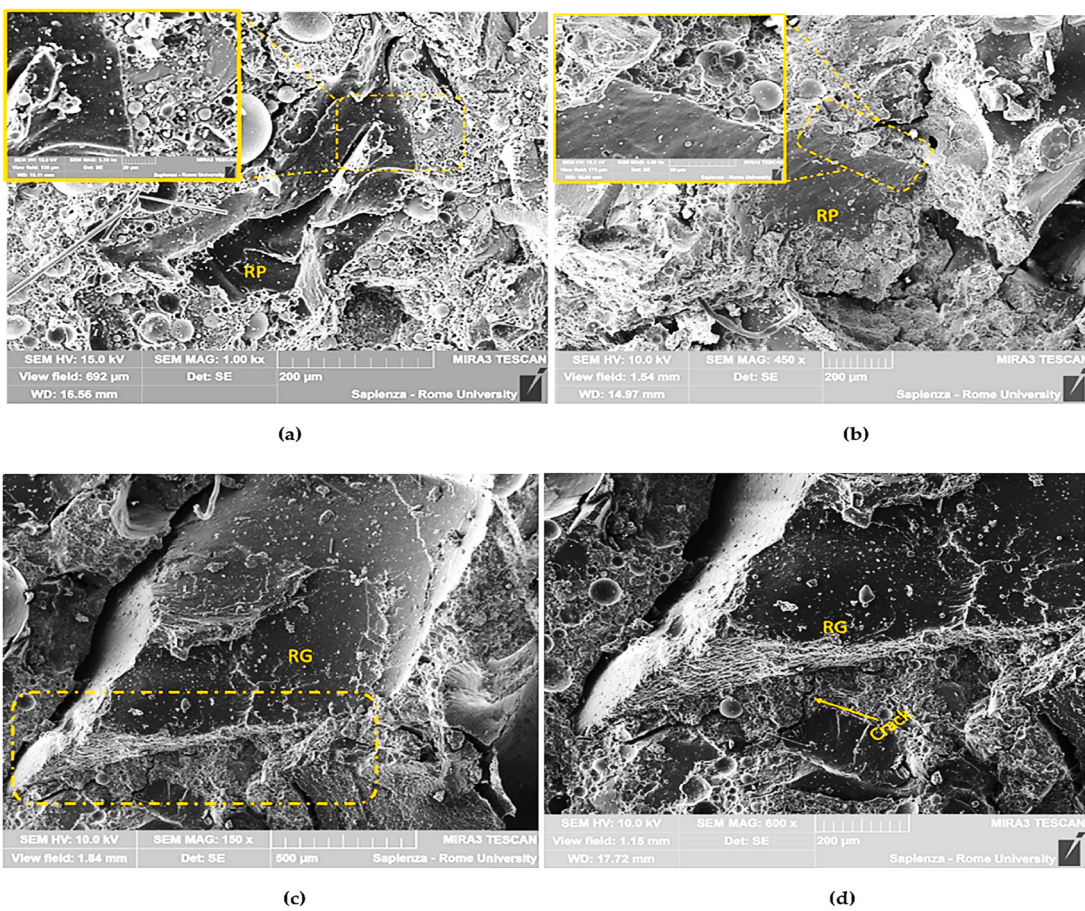


Fig. 32. Rubber-Geopolymer interface properties: RP (a-b) and RG (c-d) [160].

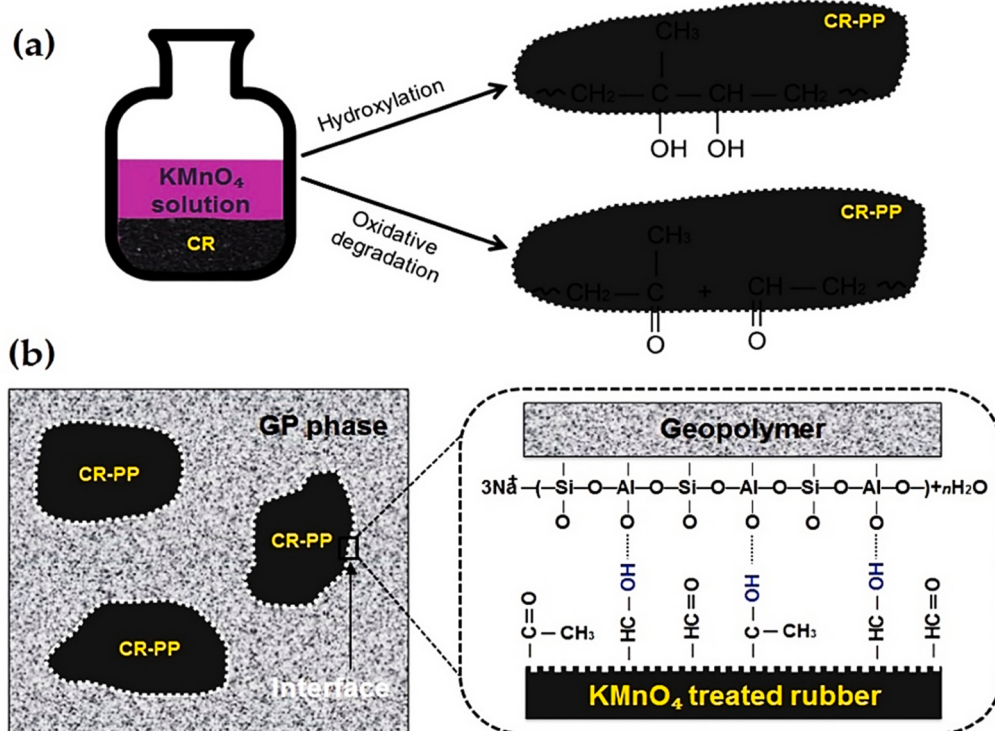


Fig. 33. (a) Reaction mechanism during the  $\text{KMnO}_4$  treatment of CRu and (b) schematic illustration of the interfacial interaction between  $\text{KMnO}_4$  treated CRu and geopolymer matrix [161].

attributable to the mix's increased porosity and decreased density as a result of the increased CRu addition, as shown in Fig. 34 [101]. Rubber particles also have a lower thermal conductivity than natural aggregate, which is even less when CRu is used instead of natural aggregate. This is even less when CRu is used instead of natural aggregate.

Thermal conductivity is also affected by the binder type. For example, when fly ash-based rubberized geopolymers mortar mixtures with 100% CRu substitution of fine aggregate were compared to rubberized concrete mixtures with the same CRu substitution, the thermal conductivity of the fly ash-based rubberized geopolymers mortar mixtures was reduced by 35% [140]. This variation in thermal conductivity results from fly ash having a lower specific gravity than PC and Ru-GPC mixtures having a larger liquid-to-solid ratio [194]. On the other hand, the resistance of concrete structures to extreme temperatures is a critical factor to consider because it can affect their chemical and physical properties [195]. Luhar, Chaudhary and Luhar [118] studied the mass loss and degradation of compressive strength in Ru-GPC samples after 2 h of exposure to elevated temperatures of up to 800 °C. As the temperature rose, a continuous mass loss was found, with more mass loss found for Ru-GPC samples than for GPC samples treated at the same temperature. Likewise, the drop in compressive strength at increasing temperatures was greater for Ru-GPC samples (52.4% at 800 °C) than for GPC samples (45.2% at 800 °C). Figs. 35 and 36 present the thermal conductivity versus CRu substitution and the relationship between thermal conductivity and density of Ru-GPC based on previous studies, respectively.

### 11.2. Sound properties

In terms of sound characteristics, it has been observed that Ru-GPC samples with up to 10% CRu substitution by weight of fine aggregate and coarse aggregate had a lower sound transmission loss than PC-concrete, as shown in Fig. 37 [117]. Yet, when fine aggregate and coarse aggregate were replaced with CRu at a ratio of 14%, the sound transmission loss coefficients were reduced to lower than that of PC-concrete. This is most likely because of the increased pores associated with increased CRu addition since sound travels quickly through porous structures. Gandoman and Kokabi [117] revealed that the sound transmission loss coefficients for Ru-GPC mixtures with 0%, 3%, and 6% CRu substitution of fine aggregate and coarse aggregate were 44.6, 45.0, and 44.1 dB, respectively, as shown in Fig. 38. While adding CRu at 10% and 14% led to sound transmission loss coefficients of 36.9 and 33 dB, respectively. However, the PC-concrete's sound transmission loss

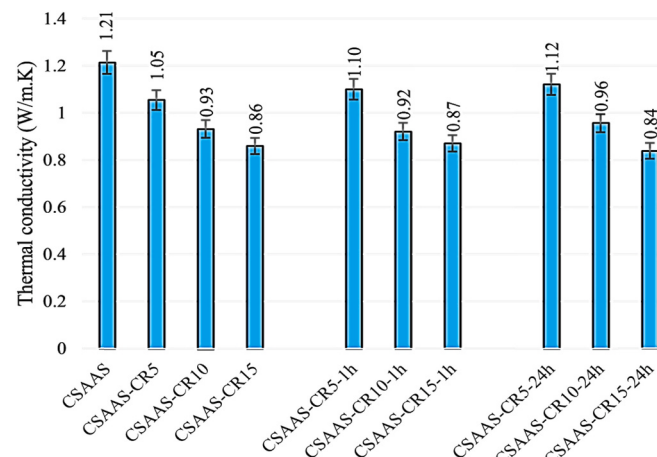


Fig. 34. Thermal conductivity at 28-d, where CSAAS-CR5 is a copper slag alkali-activated slag mortar containing 5% CRu as a partial replacement of copper slag, while CSAAS-CR5-1 h is a copper slag alkali-activated slag mortar containing 5% CRu as a partial replacement of CS alkali-treated for 1 h [101].

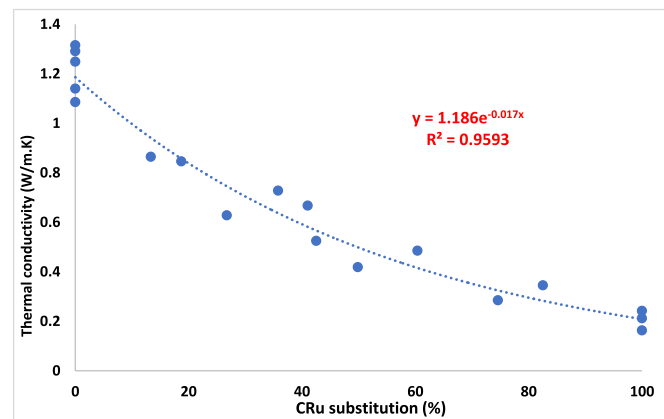


Fig. 35. The thermal conductivity of Ru-GPC versus CRu substitution [107, 140, 196, 197].

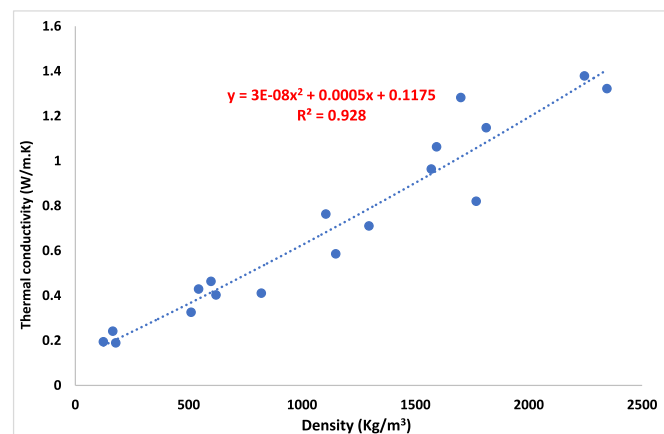


Fig. 36. The relationship between density and thermal conductivity of Ru-GPC [107, 126, 140, 196, 197].

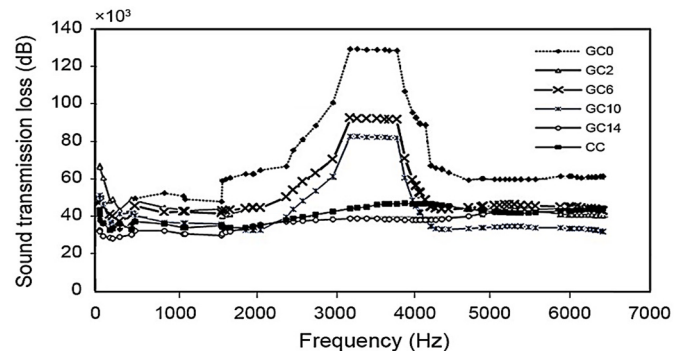
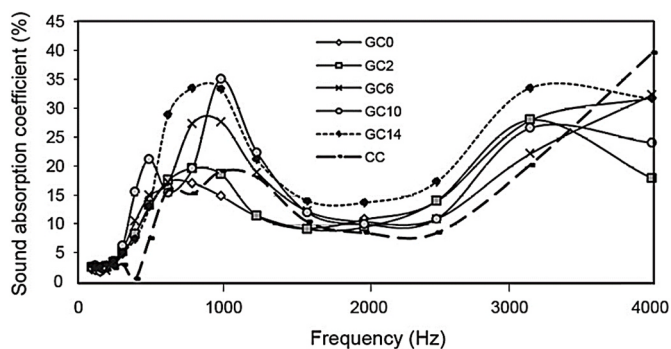
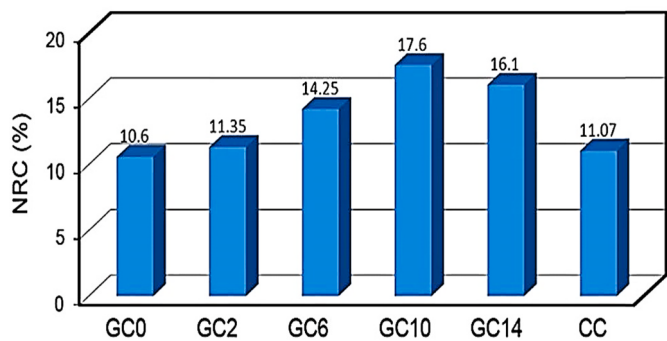


Fig. 37. Plots of sound transmission loss versus frequency for conventional and waste rubber GPC samples [117].

coefficient was 36.5 dB. Moreover, as compared to PC-concrete samples, Ru-GPC samples exhibited superior sound absorption behavior (as evaluated by non-reflected sound waves) for frequencies up to 4000 Hz [117]. Moreover, when the noise-reducing coefficient was evaluated as a function of sound absorption, the results indicated that Ru-GPC samples had a superior noise reduction coefficient (NRC) than PC-concrete samples, as shown in Fig. 39. Samples with 6% and 14% CRu substitution of fine and coarse aggregate had NRC values of 14.3 and 16.1%, respectively. PC-concrete had an NRC value of 11.1%.



**Fig. 38.** Plots of variation of sound absorption coefficients versus frequency for conventional and waste rubber GPC samples [117].



**Fig. 39.** Variation of noise reduction coefficients for conventional and waste Ru-GPC samples. Samples, i.e., GC0, GC2, GC6, GC10, and GC14, were produced by adding 0, 2, 6, 10, and 14 wt% of waste rubber based on the total aggregates [117].

## 12. Applications

After years of research, the uses of GPs and alkali-activated materials are still somewhat limited, owing to the difficulty of handling, transporting, and using liquid alkaline activators. Specific precautions are required when using such extremely corrosive ingredients properly (for example, sodium hydroxide, sodium silicate, potassium hydroxide, etc.). This results in increased utilization of solid activators, including sodium metasilicate anhydrate. On the other hand, sodium metasilicate can be utilized as a ready-to-mix mixture that looks remarkably similar to PC-concrete. By ambient temperature curing, the Illikainen research team has proven its ability to produce compressive strengths of up to 107 MPa (28-d) utilizing one-part GP [198–202]. However, geopolymeric binders and alkali-activated materials promise to be utilized as sustainable concrete materials in important infrastructure segments in either form due to their extremely high-thermal resistance of up to 1350 °C [203], approximately 75% reduction in acid resistance [204–210].

However, by incorporating CRu into GPC to make Ru-GPC, lightweight concrete with improved impact characteristics, thermal and sound insulation properties, and abrasion resistance is developed. This property makes Ru-GPC an excellent material for highway accident barriers [211], hollow blocks [130], lightweight members [212], foundation pads and rail sleepers [213], structural insulated panels [214], and thermal and sound barriers for machinery [98,215–217]. Unconfined Ru-GPC can be utilized in non-structural and pavement parts despite the loss in strength due to the increased CRu substitution [213]. Confined Ru-GPC is suitable for application in columns and bridge piers and low-to medium-rise structures in seismically active areas [85,218–220].

## 13. Embodied CO<sub>2</sub> emissions and cost analysis

Valente, Sambucci, Chougan and Ghaffar [160] analyzed the possible embodied CO<sub>2</sub> emission performance and cost analysis to assess the environmental and economic effects of using recycled rubber as a full aggregate in PC and GP mixtures. The embodied CO<sub>2</sub> findings are shown in Fig. 40-a. According to the authors, irrespective of the mixture design used in this trial, the alkali-activated materials binder (geopolymers) created in this study produced less carbon dioxide than its PC equivalent. Using the PC mixture findings as a reference, it is feasible to observe embodied CO<sub>2</sub> decrease rates of around 30% and 40% for control-alkali-activated materials and RP100alkali-activated materials mixtures (RP100 indicates 100% CRu), respectively. This result is consistent with those stated in a past study review carried out by the instigators Valente, Sambucci and Sibai [221], whereas the Alkali-Activated Materials Technology has been determined to represent a viable and environmentally sustainable alternative to conventional cement mixtures, resulting in up to an 80% reduction in carbon emissions. The carbon footprint of both matrices was expected to rise when the mineral component was replaced with tire rubber aggregate. Compared to reference formulations, the adjusted mix design exhibits an approximately 52% rise in the embodied CO<sub>2</sub> index (RP100-PC) and a 28% increase in the embodied CO<sub>2</sub> index (RP100alkali-activated materials). This tendency is not related to the environmental impact of ground tire rubber processes, which is better for the environment than using mineral aggregates, but to the increased raw material percentage needed (PC and A-S binders/alkali activator). The findings corroborate a recent life cycle assessment conducted by Maxineasa, Neocleous, Dumitrescu, Themistocleous, Taranu and Hadjimitsis [222], which established a roughly 5% increase in CO<sub>2</sub> emissions associated with the production of concrete mixtures incorporating recycled rubber particles as a partial substitute (40%). Medine, Trouzine, de Aguiar and Djadouni [223] demonstrated the opposite, demonstrating that modest replacement rates of mineral aggregates with rubber aggregates (up to 10% w/w) resulted in minor CO<sub>2</sub> emission reductions (0.25%–0.48%) when compared to a standard concrete mixture. As a result, considering a low ground tire rubber percentage would be ineffective regarding environmental effects and technical characteristics. It would be worthwhile to emphasize studies on developing more sustainable matrices that integrate a significant volume of recycled rubber. According to the embodied CO<sub>2</sub> data, ground tire rubber appears to perform better in alkali-activated material matrices, where the environmental effect is mostly due to the creation of the alkaline-activator (about 93% of the total emission contribution). In this context, by developing a “cleaner” alkali-activated materials mix design, for instance, by the use of “one-part geopolymer technology” [224], more favorable eco-sustainability levels may be obtained.

The fundamental elements utilized to create the current alkali-activated materials formulation increased the final material's manufacturing cost, as shown in Fig. 40-b, corroborating a previous study's cost analysis comparison of geopolymeric and PC-concrete materials [225,226]. Ground tire rubber's impact on cost calculations relies entirely on sand market pricing. The available data can discern two distinct tendencies: for RP100-PC mix production, rubber addition decreases aggregate fraction costs by roughly 28%, but for RP100alkali-activated materials mixture production, ground tire rubber aggregate costs 2.5 times as much as mineral aggregate. Nevertheless, caution is advised when generalizing the findings, as the study was conducted in two distinct contexts, namely British and Italian, and the aggregates' prices may vary significantly. According to previously disclosed experimental data, rubberized alkali-activated material mixes displayed comparable or better performance than cement-based materials, using fewer materials to achieve equivalent structural stability. GPs are also subject to a reduced carbon tax system, which might be used to assist with low-carbon solutions.

Moreover, due to current worldwide sustainable environmental

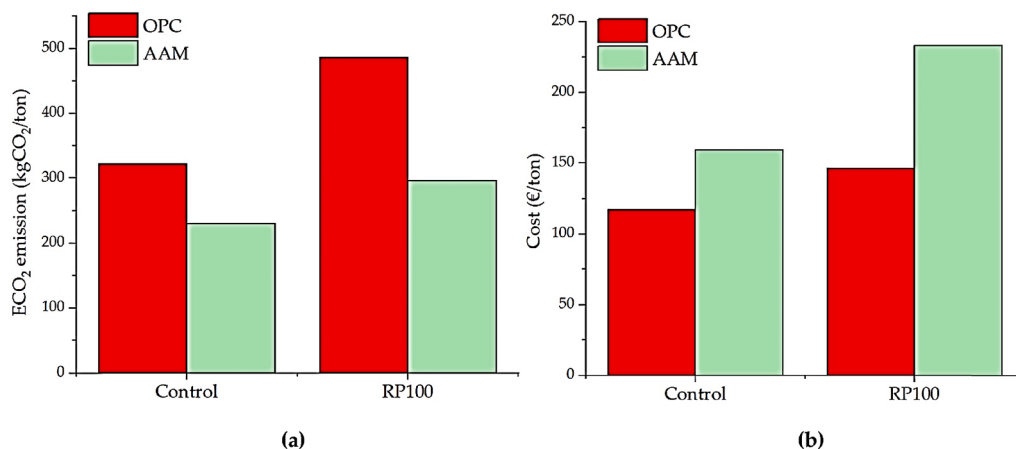


**Fig. 40.** Embodied CO<sub>2</sub> emission (a) and cost analysis (b): Comparison among normal concrete and rubberized concrete considering PC and alkali-activated materials [160].

policies focused on conserving natural resources, the cost of conventional aggregates is projected to rise in the future. Thus, the utilization of recycled rubber materials in targeted architectural and civil applications can significantly increase their functionality (lightweight precast elements, increased ductility of pavement sections, thermal-noise blocking blocks in buildings) [146]. This may be a more cost-effective alternative. These factors can narrow the cost differential between PC and GP cementitious composites.

#### 14. Conclusions

The following summarizes the review's conclusions:

1. The strength of Ru-GPC and how quickly it sets are very intricately linked to the amount of calcium oxide in the A-S precursor's chemical components.
2. Pretreating CRu particles with sodium hydroxide solution or soaking them in water can help them become adhesive to the GP mixture around them, which improves mechanical properties, increases thermal conductivity, and reduces slump.
3. For high compressive strength in Ru-GPC, the optimal SS/SH ratio is around 2, while the ideal sodium hydroxide concentration is approximately 14–15 molarity. Generally, a ratio of 0.35–0.4 is advised for the alkaline solution-to-AS precursor.
4. Oven curing is 1.5 times more efficient than steam curing for Ru-GPC. The optimum curing conditions for the oven include a heating period of up to 48 h at a temperature of 75 °C.
5. When considerable amounts of CRu were used instead of natural aggregate, the dry density dropped by up to 33.5% for 50% CRu substitution and 42% for 100% CRu substitution.
6. The substitution of high CRu for natural aggregate in Ru-GPC affects the slump/flow of the concrete, hence reducing workability. This could result in a 50% decrease in a slump with 60% CRu substitution.
7. The Ru-GPC's compressive strength reduces as the CRu content is increased. Compressive strength is reduced by 63% when 30% CRu is substituted for 100% natural aggregate. Compressive strength is reduced by more than 80% at sustainable levels of roughly 60%.
8. The compressive strength, splitting tensile strength, flexural strength, and MOE of natural aggregate decrease as the CRu substitution increases. Moreover, there is a substantial relationship between splitting tensile strength and flexural strength.
9. Compared to non-rubberized concrete samples, Ru-GPC samples stay intact under high strain levels and have a higher dynamic increase factor than GPC samples. Moreover, Ru-GPC disc

samples exhibited advantageous ductile failure processes upon impact.

10. Ru-GPC samples become more porous and water-absorbing as the CRu substitution of natural aggregates increases, which means that the samples get better. When 100% CRu is used instead of natural aggregate, water absorption can rise by up to 2.5 times.
11. Increased CRu substitution for natural aggregate results in increased drying shrinkage because of the lower restriction provided by CRu particles compared to natural aggregate. The thermal conductivity of Ru-GPC samples reduces when more CRu is substituted for natural aggregate, achieving a maximum of 82% with 100% CRu substitution. Moreover, there is a clear relationship between the thermal conductivity of Ru-GPC samples and their density.

#### 15. Recommendations

1. There are presently no studies on structural members employing Ru-GPC materials that have been subjected to various forms of loading. Additional studies are required to fully comprehend and quantify Ru-GPC structural components' behavior.
2. Presently, no research has been done on the fresh properties of GGBFS-based rubberized alkali-activated concrete.
3. Until now, the study of the behavior of rubberized one-part GPC has been extremely restricted. Basic investigations into the materials and structural behavior of such materials are required.
4. Most past research on Ru-GPC materials has concentrated on two-part GPC. One-part GPC, where the alkaline-activator is mixed solidly with the dry precursors and then water is added, is another option.
5. Another unexplored area of study on Ru-GPC is improving the compatibility of CRu particles with the GP matrix to minimize bond issues.
6. In terms of durability, no research has been done on how Ru-GPC behaves under long-term loading, and most of the data on carbonation depth, shrinkage, sorptivity, efflorescence, freeze-thaw resistance, sulfate resistance, and rebar corrosion are mostly inadequate.
7. To make Ru-GPC flexible and useful in many situations, it is important to evaluate the full range of stress-strain responses and create foundational models for design goals.

#### Declaration of competing interest

The authors declare that they have no known competing financial interests or personal relationships that could have appeared to influence the work reported in this paper.

## Acknowledgement

The authors are thankful to the Deanship of Scientific Research at Najran University for funding this work under the Research Collaboration Funding program grant code (NU/RC/SERC/11/1).

## References

- [1] R. Siddique, T.R. Naik, Properties of concrete containing scrap-tire rubber—an overview, *Waste Manag.* 24 (2004) 563–569.
- [2] W. Shen, L. Shan, T. Zhang, H. Ma, Z. Cai, H. Shi, Investigation on polymer-rubber aggregate modified porous concrete, *Construct. Build. Mater.* 38 (2013) 667–674.
- [3] F. Azevedo, F. Pacheco-Torgal, C. Jesus, J.B. De Aguiar, A. Camões, Properties and durability of HPC with tyre rubber wastes, *Construct. Build. Mater.* 34 (2012) 186–191.
- [4] J. Eiras, F. Segovia, M. Borrachero, J. Monzó, M. Bonilla, J. Payá, Physical and mechanical properties of foamed Portland cement composite containing crumb rubber from worn tires, *Mater. Des.* 59 (2014) 550–557.
- [5] S. Kaza, L. Yao, P. Bhada-Tata, F. Van Woerden, What a Waste 2.0: A Global Snapshot of Solid Waste Management to 2050, World Bank Publications, 2018.
- [6] R.M. Association, US Scrap Tire Management Summary, Rubber Manufacturers Association, 2014.
- [7] A.R.G. de Azevedo, J. Alexandre, G.d.C. Xavier, L.G. Pedroti, Recycling paper industry effluent sludge for use in mortars: a sustainability perspective, *J. Clean. Prod.* 192 (2018) 335–346.
- [8] Y. Park, A. Abolmaali, M. Mohammadagha, S. Lee, Structural performance of dry-cast rubberized concrete pipes with steel and synthetic fibers, *Construct. Build. Mater.* 77 (2015) 218–226.
- [9] B.S. Mohammed, K.M.A. Hossain, J.T.E. Swee, G. Wong, M. Abdullahi, Properties of crumb rubber hollow concrete block, *J. Clean. Prod.* 23 (2012) 57–67.
- [10] X. He, Z. Yuhua, S. Qaidi, H.F. Isleem, O. Zaid, F. Althoey, J. Ahmad, Mine tailings-based geopolymers: a comprehensive review, *Ceram. Int.* (2022).
- [11] H.A. Toutanji, The use of rubber tire particles in concrete to replace mineral aggregates, *Cement Concr. Compos.* 18 (1996) 135–139.
- [12] Z.K. Khatib, F.M. Bayomy, Rubberized Portland cement concrete, *J. Mater. Civ. Eng.* 11 (1999) 206–213.
- [13] C.A. Issa, G. Salem, Utilization of recycled crumb rubber as fine aggregates in concrete mix design, *Construct. Build. Mater.* 42 (2013) 48–52.
- [14] Y. Park, A. Abolmaali, M. Mohammadagha, S.-H. Lee, Flexural characteristic of rubberized hybrid concrete reinforced with steel and synthetic fibers, *Adv. Civil. Eng. Mater.* 3 (2014) 495–508.
- [15] F. Pacheco-Torgal, Introduction to Handbook of Alkali-Activated Cements, Mortars and Concretes, Handbook of Alkali-Activated Cements, Mortars and Concretes, Elsevier, 2015, pp. 1–16.
- [16] F.A. Jawad Ahmad, Rebeca Martinez-Garcia, Jesús de-Prado-Gil, M. Shaker, A. Qaidi, Ameni Brahmia, Effects of waste glass and waste marble on mechanical and durability performance of concrete, *Sci. Rep.* 11 (2021), 21525.
- [17] A. Mansi, N.H. Sor, N. Hilal, S.M. Qaidi, The Impact of Nano Clay on Normal and High-Performance Concrete Characteristics: A Review, IOP Conference Series: Earth and Environmental Science, IOP Publishing, 2022, 012085.
- [18] E.I. Diaz-Loya, E.N. Allouche, S. Vaidya, Mechanical properties of fly-ash-based geopolymer concrete, *ACI Mater. J.* 108 (2011) 300.
- [19] M.M. Al Bakri, H. Mohammed, H. Kamardin, I.K. Niza, Y. Zarina, Review on fly ash-based geopolymer concrete without Portland Cement, *J. Eng. Technol. Res.* 3 (2011) 1–4.
- [20] S.M.A. Qaidi, B.A. Tayeh, A.M. Zeyad, A.R.G. de Azevedo, H.U. Ahmed, W. Emad, Recycling of Mine Tailings for the Geopolymers Production: A Systematic Review, Case Studies in Construction Materials, 2022.
- [21] S.M.A. Qaidi, Y.Z. Dinkha, J.H. Haido, M.H. Ali, B.A. Tayeh, Engineering properties of sustainable green concrete incorporating eco-friendly aggregate of crumb rubber: a review, *J. Clean. Prod.* (2021), 129251.
- [22] H.U. Ahmed, A.A. Mohammed, S. Rafiq, A.S. Mohammed, A. Mosavi, N.H. Sor, S. Qaidi, Compressive strength of sustainable geopolymer concrete composites: a state-of-the-art review, *Sustainability* 13 (2021), 13502.
- [23] J. Davidovits, Chemistry of Geopolymeric Systems, Terminology, Geopolymer, sn, 1999, pp. 9–39.
- [24] D. Hardjito, S.E. Wallah, D.M. Sumajouw, B.V. Rangan, On the development of fly ash-based geopolymer concrete, *J. Mater.* 101 (2004) 467–472.
- [25] A. Siddika, M.A.A. Mamun, R. Alyousef, Y.H.M. Amran, F. Aslani, H. Alabduljabbar, Properties and utilizations of waste tire rubber in concrete: a review, *Construct. Build. Mater.* 224 (2019) 711–731.
- [26] ETRMA, End of Life Tyres Management – Europe – 2019, European Tyre and Rubber Manufacturers' Association, 2021.
- [27] P. Zhang, K. Wang, Q. Li, J. Wang, Y. Ling, Fabrication and engineering properties of concretes based on geopolymers/alkali-activated binders-A review, *J. Clean. Prod.* 258 (2020), 120896.
- [28] W.S. Alaloul, M.A. Musarat, B.A. Tayeh, S. Sivalingam, M.F.B. Rosli, S. Haruna, M.I. Khan, Mechanical and deformation properties of rubberized engineered cementitious composite (ECC), *Case Stud. Constr. Mater.* 13 (2020), e00385.
- [29] P. Psyllaki, K. Stamatou, I. Iliadis, A. Mourlas, P. Asteris, N. Vaxevanidis, Surface treatment of tool steels against galling failure, in: MATEC Web of Conferences, vol. 188, EDP Sciences, 2018, 04024.
- [30] P.G. Asteris, E. Gavrilaki, T. Touloudenidou, E.E. Koravou, M. Koutra, P. G. Papayanni, A. Anagnostopoulos, Genetic prediction of ICU hospitalization and mortality in COVID-19 patients using artificial neural networks, *J. Cell Mol. Med.* 26 (5) (2022) 1445–1455.
- [31] P.G. Asteris, P.B. Lourenço, M. Hajihassani, C.E.N. Adami, M.E. Lemonis, A. D. Skentou, H. Varum, Soft computing-based models for the prediction of masonry compressive strength, *Eng. Struct.* 248 (2021), 113276.
- [32] P.G. Asteris, P.B. Lourenço, P.C. Roussis, C.E. Adami, D.J. Armaghani, L. Cavalieri, K. Pilakoutas, Revealing the nature of metakaolin-based concrete materials using artificial intelligence techniques, *Construct. Build. Mater.* 322 (2022), 126500.
- [33] P.G. Asteris, M. Apostolopoulou, D.J. Armaghani, L. Cavalieri, A.T. Chountalas, D. Guney, H. Nguyen, On the metaheuristic models for the prediction of cement-metakaolin mortars compressive strength, 1, 1, 2020, 063.
- [34] A. Bardhan, R. Biswas, N. Kardani, M. Iqbal, P. Samui, M.P. Singh, P.G. Asteris, A novel integrated approach of augmented grey wolf optimizer and ANN for estimating axial load carrying-capacity of concrete-filled steel tube columns, *Construct. Build. Mater.* 337 (2022), 127454.
- [35] M. Koopalipoor, P.G. Asteris, A.S. Mohammed, D.E. Alexakis, A. Mamou, D. J. Armaghani, Introducing stacking machine learning approaches for the prediction of rock deformation, *Transportation Geotechnics* 34 (2022), 100756.
- [36] M.E. Lemonis, G.D. Hatzigeorgiou, P.G. Asteris, Seismic behaviour of irregular steel frames with beam and joint energy dissipation, *Soil Dynam. Earthq. Eng.* 152 (2022), 107052.
- [37] O. Zaid, F.M. Mukhtar, M. Rebeca, M.G. El Sherbiny, A.M. Mohamed, Characteristics of high-performance steel fiber reinforced recycled aggregate concrete utilizing mineral filler, *Case Stud. Constr. Mater.* 16 (2022), e00939.
- [38] Z. He, H. Nguyen, T.H. Vu, J. Zhou, P.G. Asteris, A. Mammou, Novel integrated approaches for predicting the compressibility of clay using cascade forward neural networks optimized by swarm-and evolution-based algorithms, *Acta Geotechnica* 17 (4) (2022) 1257–1272.
- [39] M. Menegaki, D. Damigos, A review on current situation and challenges of construction and demolition waste management, *Current Opinion in Green and Sustainable Chemistry* 13 (2018) 8–15.
- [40] P. Yadav, S.R. Samadder, A critical review of the life cycle assessment studies on solid waste management in Asian countries, *J. Clean. Prod.* 185 (2018) 492–515.
- [41] T. Dutta, K.-H. Kim, A. Deep, J.E. Szulejko, K. Vellingiri, S. Kumar, E.E. Kwon, S.-T. Yun, Recovery of nanomaterials from battery and electronic wastes: a new paradigm of environmental waste management, *Renew. Sustain. Energy Rev.* 82 (2018) 3694–3704.
- [42] R. Nisticò, Aquatic-derived biomaterials for a sustainable future: a European opportunity, *Resources* 6 (2017) 65.
- [43] R. Nisticò, L. Lavagna, D. Versaci, P. Ivanchenko, P. Benzi, Chitosan and its char as fillers in cement-base composites: a case study, *Bol. Soc. Espanola Ceram. Vidr.* 59 (2020) 186–192.
- [44] M. Sienkiewicz, J. Kucinska-Lipka, H. Janik, A. Balas, Progress in used tyres management in the European Union: a review, *Waste Manag.* 32 (2012) 1742–1751.
- [45] A.M. Rashad, A comprehensive overview about recycling rubber as fine aggregate replacement in traditional cementitious materials, *Int. J. Sustain. Built. Env.* 5 (2016) 46–82.
- [46] K.B. Najim, M.R. Hall, A review of the fresh/hardened properties and applications for plain- (PRC) and self-compacting rubberised concrete (SCRC), *Construct. Build. Mater.* 24 (2010) 2043–2051.
- [47] S.M.A. Qaidi, Y.S.S. Al-Kamaki, State-of-the-Art review: concrete made of recycled waste PET as fine aggregate, *J. Donghua Univ.* 23 (2021) 412–429.
- [48] S.N. Ahmed, N. Hamah Sor, M.A. Ahmed, S.M.A. Qaidi, Thermal conductivity and hardened behavior of eco-friendly concrete incorporating waste polypropylene as fine aggregate, *Mater. Today Proc.* 57 (2022) 818–823.
- [49] M.V. Cardo, P. Rosín, A.E. Carabajo, D. Vezzani, Artificial container mosquitoes and first record of Aedes aegypti in the islands of the Paraná Lower Delta, Argentina, *J. Asia Pac. Entomol.* 18 (2015) 727–733.
- [50] E. Aylón, R. Murillo, A. Fernández-Colino, A. Aranda, T. García, M.S. Callén, A. M. Mastral, Emissions from the combustion of gas-phase products at tyre pyrolysis, *J. Anal. Appl. Pyrol.* 79 (2007) 210–214.
- [51] R.H. Faraj, H.U. Ahmed, S. Rafiq, N.H. Sor, D.F. Ibrahim, S.M.A. Qaidi, Performance of self-compacting mortars modified with nanoparticles: a systematic review and modeling, *Cleaner Mater.* (2022), 100086.
- [52] I. Almeshal, M.M. Al-Tayeb, S.M.A. Qaidi, B.H. Abu Bakar, B.A. Tayeh, Mechanical properties of eco-friendly cements-based glass powder in aggressive medium, *Mater. Today Proc.* (2022).
- [53] R. Siddique, T.R. Naik, Properties of concrete containing scrap-tire rubber – an overview, *Waste Manag.* 24 (2004) 563–569.
- [54] H.U. Ahmed, A.S. Mohammed, R.H. Faraj, S.M.A. Qaidi, A.A. Mohammed, Compressive strength of geopolymer concrete modified with nano-silica: experimental and modeling investigations, *Case Stud. Constr. Mater.* 16 (2022), e01036.
- [55] H.U. Ahmed, A.A. Mohammed, S. Rafiq, A.S. Mohammed, A. Mosavi, N.H. Sor, S. M.A. Qaidi, Compressive strength of sustainable geopolymer concrete composites: a state-of-the-art review, *Sustainability* 13 (2021), 13502.
- [56] Q. Dong, B. Huang, X. Shu, Rubber modified concrete improved by chemically active coating and silane coupling agent, *Construct. Build. Mater.* 48 (2013) 116–123.
- [57] S.M.A. Qaidi, B.A. Tayeh, A.M. Zeyad, A.R.G. de Azevedo, H.U. Ahmed, W. Emad, Recycling of mine tailings for the geopolymers production: a systematic review, *Case Stud. Constr. Mater.* 16 (2022), e00933.

- [58] S.M.A. Qaidi, B.A. Tayeh, H.F. Isleem, A.R.G. de Azevedo, H.U. Ahmed, W. Emad, Sustainable utilization of red mud waste (bauxite residue) and slag for the production of geopolymer composites: a review, *Case Stud. Constr. Mater.* 16 (2022), e00994.
- [59] Research-and-Markets, Tire Recycling Downstream Products - Global Market Outlook (2019-2027), 2020.
- [60] N.N. Gerges, C.A. Issa, S.A. Fawaz, Rubber concrete: mechanical and dynamical properties, *Case Stud. Constr. Mater.* 9 (2018), e00184.
- [61] V. Goodship, Management, Recycling and Reuse of Waste Composites, first ed., Elsevier Science, 2009.
- [62] K.C. Baranwal, Akron Rubber Development Laboratory, Rubber Division Meeting of the American Chemical Society, ASTM Standards and Testing of Recycle Rubber, San Francisco, Calif., 2003.
- [63] S. Ramarad, M. Khalid, C.T. Ratnam, A.L. Chuah, W. Rashmi, Waste tire rubber in polymer blends: a review on the evolution, properties and future, *Prog. Mater. Sci.* 72 (2015) 100–140.
- [64] S. Herrero, P. Mayor, F. Hernández-Olivares, Influence of proportion and particle size gradation of rubber from end-of-life tires on mechanical, thermal and acoustic properties of plaster-rubber mortars, *Mater. Des.* 47 (2013) 633–642.
- [65] L. Li, S. Ruan, L. Zeng, Mechanical properties and constitutive equations of concrete containing a low volume of tire rubber particles, *Construct. Build. Mater.* 70 (2014) 291–308.
- [66] S.M.A. Qaidi, Behavior of Concrete Made of Recycled PET Waste and Confined with CFRP Fabrics, College of Engineering, University of Duhok, 2021.
- [67] A. Caggiano, H. Xargay, P. Folino, E. Martinelli, Experimental and numerical characterization of the bond behavior of steel fibers recovered from waste tires embedded in cementitious matrices, *Cement Concr. Compos.* 62 (2015) 146–155.
- [68] E. Ganjian, M. Khorami, A.A. Maghsoudi, Scrap-tire-rubber replacement for aggregate and filler in concrete, *Construct. Build. Mater.* 23 (2009) 1828–1836.
- [69] A. Pehlken, K.-D. Thoben, Contribution of Recycling Processes to Sustainable Resource Management, Glocalized Solutions for Sustainability in Manufacturing, Springer, 2011, pp. 465–469.
- [70] R.A. Assaggaf, M.R. Ali, S.U. Al-Dulaijan, M. Maslehuddin, Properties of concrete with untreated and treated crumb rubber – a review, *J. Mater. Res. Technol.* 11 (2021) 1753–1798.
- [71] S. Hesami, I. Salehi Hikouei, S.A.A. Emadi, Mechanical behavior of self-compacting concrete pavements incorporating recycled tire rubber crumb and reinforced with polypropylene fiber, *J. Clean. Prod.* 133 (2016) 228–234.
- [72] B.S. Thomas, R.C. Gupta, V.J. Panicker, Recycling of waste tire rubber as aggregate in concrete: durability-related performance, *J. Clean. Prod.* 112 (2016) 504–513.
- [73] I. Mohammadi, H. Khabbaz, K. Vessalas, In-depth assessment of Crumb Rubber Concrete (CRC) prepared by water-soaking treatment method for rigid pavements, *Construct. Build. Mater.* 71 (2014) 456–471.
- [74] B. Li, H. Li, Y. Wei, X. Zhang, D. Wei, J. Li, Microscopic properties of hydrogen peroxide activated crumb rubber and its influence on the rheological properties of crumb rubber modified asphalt, *Materials* 12 (2019) 1434.
- [75] Y.-c. Guo, J.-h. Zhang, G.-m. Chen, Z.-h. Xie, Compressive behaviour of concrete structures incorporating recycled concrete aggregates, rubber crumb and reinforced with steel fibre, subjected to elevated temperatures, *J. Clean. Prod.* 72 (2014) 193–203.
- [76] J. Xie, J. Li, Z. Lu, Z. Li, C. Fang, L. Huang, L. Li, Combination effects of rubber and silica fume on the fracture behaviour of steel-fibre recycled aggregate concrete, *Construct. Build. Mater.* 203 (2019) 164–173.
- [77] J. Xie, Y. Zheng, Y. Guo, R. Ou, Z. Xie, L. Huang, Effects of crumb rubber aggregate on the static and fatigue performance of reinforced concrete slabs, *Compos. Struct.* 228 (2019), 111371.
- [78] L. He, Y. Ma, Q. Liu, Y. Mu, Surface modification of crumb rubber and its influence on the mechanical properties of rubber-cement concrete, *Construct. Build. Mater.* 120 (2016) 403–407.
- [79] C. Xiaowei, H. Sheng, G. Xiaoyang, D. Wenhui, Crumb waste tire rubber surface modification by plasma polymerization of ethanol and its application on oil-well cement, *Appl. Surf. Sci.* 409 (2017) 325–342.
- [80] C.-Y. Chen, M.-T. Lee, Application of crumb rubber in cement-matrix composite, *Materials* 12 (2019) 529.
- [81] H. Zhang, M. Gou, X. Liu, X. Guan, Effect of rubber particle modification on properties of rubberized concrete, *J. Wuhan Univ. Technol.-Materials Sci. Ed.* 29 (2014) 763–768.
- [82] J.O. Akinyele, R.W. Salim, W.K. Kupolati, The impact of rubber crumb on the mechanical and chemical properties of concrete, *Eng. Struct. Technol.* 7 (2015) 197–204.
- [83] İ.B. Topcu, A. Unverdi, 2 - scrap tires/crumb rubber, in: R. Siddique, P. Cachim (Eds.), Waste and Supplementary Cementitious Materials in Concrete, Woodhead Publishing, 2018, pp. 51–77.
- [84] C. Chen, R. Zhang, L. Zhou, Y. Wang, Influence of waste tire particles on freeze-thaw resistance and impermeability performance of waste tires/sand-based autoclaved aerated concrete composites, *Buildings* 12 (2022) 33.
- [85] O. Youssif, R. Hassanli, J.E. Mills, Retrofitting square columns using FRP-confined crumb rubber concrete to improve confinement efficiency, *Construct. Build. Mater.* 153 (2017) 146–156.
- [86] K.B. Najim, M.R. Hall, Mechanical and dynamic properties of self-compacting crumb rubber modified concrete, *Construct. Build. Mater.* 27 (2012) 521–530.
- [87] S. Raffoul, R. Garcia, D. Escalano-Margarit, M. Guadagnini, I. Hajirasouliha, K. Pilakoutas, Behaviour of unconfined and FRP-confined rubberised concrete in axial compression, *Construct. Build. Mater.* 147 (2017) 388–397.
- [88] T. Gupta, S. Chaudhary, R.K. Sharma, Assessment of mechanical and durability properties of concrete containing waste rubber tire as fine aggregate, *Construct. Build. Mater.* 73 (2014) 562–574.
- [89] A.F. Angelin, F.M. Da Silva, L.A.G. Barbosa, R.C.C. Lintz, M.A.G. De Carvalho, R. A.S. Franco, Voids identification in rubberized mortar digital images using K-Means and Watershed algorithms, *J. Clean. Prod.* 164 (2017) 455–464.
- [90] J.H. Chen, K.S. Chen, L.Y. Tong, On the pyrolysis kinetics of scrap automotive tires, *J. Hazard Mater.* 84 (2001) 43–55.
- [91] F. Aslani, G. Ma, D.L. Yim Wan, V.X. Tran Le, Experimental investigation into rubber granules and their effects on the fresh and hardened properties of self-compacting concrete, *J. Clean. Prod.* 172 (2018) 1835–1847.
- [92] B. Muñoz-Sánchez, M.J. Arévalo-Caballero, M.C. Pacheco-Menor, Influence of acetic acid and calcium hydroxide treatments of rubber waste on the properties of rubberized mortars, *Mater. Struct.* 50 (2016) 75.
- [93] E. Fraile-García, J. Ferreiro-Cabello, M. Mendivil-Giro, A.S. Vicente-Navarro, Thermal behaviour of hollow blocks and bricks made of concrete doped with waste tyre rubber, *Construct. Build. Mater.* 176 (2018) 193–200.
- [94] B. Singh, G. Ishwarya, M. Gupta, S. Bhattacharyya, Geopolymer concrete: a review of some recent developments, *Construct. Build. Mater.* 85 (2015) 78–90.
- [95] H. Zhong, E.W. Poon, K. Chen, M. Zhang, Engineering properties of crumb rubber alkali-activated mortar reinforced with recycled steel fibres, *J. Clean. Prod.* 238 (2019), 117950.
- [96] A.M. Rashad, D.M. Sadek, Behavior of alkali-activated slag pastes blended with waste rubber powder under the effect of freeze/thaw cycles and severe sulfate attack, *Construct. Build. Mater.* 265 (2020), 120716.
- [97] F. Sajedi, H.A. Razak, Comparison of different methods for activation of ordinary Portland cement-slag mortars, *Construct. Build. Mater.* 25 (2011) 30–38.
- [98] F. Aslani, A. Deghani, Z. Asif, Development of lightweight rubberized geopolymer concrete by using polystyrene and recycled crumb-rubber aggregates, *J. Mater. Civ. Eng.* 32 (2020), 04019345.
- [99] Q.-H. Lương, H.H. Nguyễn, J.-I. Choi, H.-K. Kim, B.Y. Lee, Effects of crumb rubber particles on mechanical properties and sustainability of ultra-high-ductile slag-based composites, *Construct. Build. Mater.* 272 (2021), 121959.
- [100] W.-J. Long, H.-D. Li, J.-J. Wei, F. Xing, N. Han, Sustainable use of recycled crumb rubbers in eco-friendly alkali activated slag mortar: dynamic mechanical properties, *J. Clean. Prod.* 204 (2018) 1004–1015.
- [101] F. Ameri, P. Shoaei, H.R. Musaei, S.A. Zareei, C.B. Cheah, Partial replacement of copper slag with treated crumb rubber aggregates in alkali-activated slag mortar, *Construct. Build. Mater.* 256 (2020), 119468.
- [102] Y. Park, A. Abolmaali, Y.H. Kim, M. Ghahremannejad, Compressive strength of fly ash-based geopolymer concrete with crumb rubber partially replacing sand, *Construct. Build. Mater.* 118 (2016) 43–51.
- [103] Z. Yahya, M. Abdullah, S. Ramli, M. Minciuna, R. Abd Razak, Durability of fly ash based geopolymer concrete infilled with rubber crumb in seawater exposure, in: IOP Conference Series: Materials Science and Engineering, IOP Publishing, 2018, 012069.
- [104] A.A. Azmi, M.M.A.B. Abdullah, C.M.R. Ghazali, A.V. Sandu, K. Hussin, Effect of Crumb Rubber on Compressive Strength of Fly Ash Based Geopolymer Concrete, MATEC Web of Conferences, EDP Sciences, 2016, 01063.
- [105] M. Rajendran, M. Akasi, Performance of crumb rubber and nano fly ash based ferro-geopolymer panels under impact load, *KSCE J. Civ. Eng.* 24 (2020) 1810–1820.
- [106] M. Dong, M. Elchalakani, A. Karrech, B. Yang, Strength and durability of geopolymer concrete with high volume rubber replacement, *Construct. Build. Mater.* 274 (2021), 121783.
- [107] A. Wongsa, V. Sata, B. Nematollahi, J. Sanjayan, P. Chindaprasirt, Mechanical and thermal properties of lightweight geopolymer mortar incorporating crumb rubber, *J. Clean. Prod.* 195 (2018) 1069–1080.
- [108] G. Mucci, Á. Szenczi, S. Nagy, Fiber reinforced geopolymer from synergistic utilization of fly ash and waste tire, *J. Clean. Prod.* 178 (2018) 429–440.
- [109] P.E. Pavithra, M.S. Reddy, P. Dinakar, B.H. Rao, B. Satpathy, A. Mohanty, A mix design procedure for geopolymer concrete with fly ash, *J. Clean. Prod.* 133 (2016) 117–125.
- [110] Y.M. Amran, R. Alyousef, H. Alabduljabbar, M. El-Zeadani, Clean production and properties of geopolymer concrete; A review, *J. Clean. Prod.* 251 (2020), 119679.
- [111] P. Chindaprasirt, C. Ridtrud, High calcium fly ash geopolymer containing natural rubber latex as additive, *J. GEOMATE* 18 (2020) 124–129.
- [112] A.M. Al Bakri, H. Kamarudin, M. Bnhussain, I.K. Nizar, A. Rafiza, Y. Zarina, Microstructure of different NaOH molarity of fly ash-based green polymeric cement, *J. Eng. Technol. Res.* 3 (2011) 44–49.
- [113] D. Hardjito, B.V. Rangan, Development and Properties of Low-Calcium Fly Ash-Based Geopolymer Concrete, 2005.
- [114] R.M. Hamidi, Z. Man, K.A. Azizli, Concentration of NaOH and the effect on the properties of fly ash based geopolymer, *Procedia Eng.* 148 (2016) 189–193.
- [115] H.E. Elyamany, M. Abd Elmoaty, A.M. Elshaboury, Setting time and 7-day strength of geopolymer mortar with various binders, *Construct. Build. Mater.* 187 (2018) 974–983.
- [116] A.M. Aly, M. El-Feky, M. Kohail, E.-S.A. Nasr, Performance of geopolymer concrete containing recycled rubber, *Construct. Build. Mater.* 207 (2019) 136–144.
- [117] M. Gandoman, M. Kokabi, Sound barrier properties of sustainable waste rubber/geopolymer concretes, *Iran. Polym. J. (Engl. Ed.)* 24 (2015) 105–112.
- [118] S. Luhar, S. Chaudhary, I. Luhar, Thermal resistance of fly ash based rubberized geopolymer concrete, *J. Build. Eng.* 19 (2018) 420–428.

- [119] P. Nuaklong, P. Jongvivatskul, T. Pothisiri, V. Sata, P. Chindaprasirt, Influence of rice husk ash on mechanical properties and fire resistance of recycled aggregate high-calcium fly ash geopolymers concrete, *J. Clean. Prod.* 252 (2020), 119797.
- [120] S.C. Moghaddam, R. Madandoust, M. Jamshidi, I.M. Nikbin, Mechanical properties of fly ash-based geopolymers concrete with crumb rubber and steel fiber under ambient and sulfuric acid conditions, *Construct. Build. Mater.* 281 (2021), 122571.
- [121] S. Luhar, S. Chaudhary, I. Luhar, Development of rubberized geopolymers concrete: strength and durability studies, *Construct. Build. Mater.* 204 (2019) 740–753.
- [122] T.M. Pham, J. Liu, P. Tran, V.-L. Pang, F. Shi, W. Chen, H. Hao, T.M. Tran, Dynamic compressive properties of lightweight rubberized geopolymers concrete, *Construct. Build. Mater.* 265 (2020), 120753.
- [123] A.A. Azmi, M.M.A.B. Abdullah, C.M.R. Ghazali, R. Ahmad, L. Musa, L.S. Rou, The effect of different crumb rubber loading on the properties of fly ash-based geopolymers concrete, in: IOP Conference Series: Materials Science and Engineering, IOP Publishing, 2019, 012079.
- [124] I.M. Ali, A.S. Naje, M.S. Nasr, Eco-friendly chopped tire rubber as reinforcements in fly ash based geopolymers concrete, *Glob. Nest J.* 22 (2020) 342–347.
- [125] P.K. Dehdezi, S. Erdem, M.A. Blankson, Physico-mechanical, microstructural and dynamic properties of newly developed artificial fly ash based lightweight aggregate–Rubber concrete composite, *Compos. B Eng.* 79 (2015) 451–455.
- [126] S. Rajaei, P. Shoaei, M. Sharifiati, F. Ameri, H.R. Musaei, B. Behforouz, J. de Brito, RETRACTED: Rubberized Alkali-Activated Slag Mortar Reinforced with Polypropylene Fibres for Application in Lightweight Thermal Insulating Materials, Elsevier, 2021.
- [127] A.A. Azmi, M.M.A. Al Bakri, C.M.R. Ghazali, A.V. Sandu, K. Hussin, D.A. Sumarto, A Review on Fly Ash Based Geopolymer Rubberized Concrete, Key Engineering Materials, Trans Tech Publ, 2016, pp. 183–196.
- [128] S. Luhar, S. Chaudhary, U. Dave, Effect of different parameters on the compressive strength of rubberized geopolymers concrete, *Multi-Disciplinary Sustainable Engineering: Current and Future Trends* (2016) 77–86.
- [129] S. Luhar, I. Luhar, Rubberized geopolymers concrete: application of taguchi method for various factors, *Int. J. Recent Technol. Eng.* 8 (2020) 1167–1174.
- [130] B.S. Mohammed, M.S. Liew, W.S. Alaloul, A. Al-Fakih, W. Ibrahim, M. Adamu, Development of rubberized geopolymers interlocking bricks, *Case Stud. Constr. Mater.* 8 (2018) 401–408.
- [131] M. Palacios, Y.F. Houst, P. Bowen, F. Puertas, Adsorption of superplasticizer admixtures on alkali-activated slag pastes, *Cement Concr. Res.* 39 (2009) 670–677.
- [132] B. Nematollahi, J. Sanjayan, Effect of different superplasticizers and activator combinations on workability and strength of fly ash based geopolymers, *Mater. Des.* 57 (2014) 667–672.
- [133] M. Palacios, F. Puertas, Effect of superplasticizer and shrinkage-reducing admixtures on alkali-activated slag pastes and mortars, *Cement Concr. Res.* 35 (2005) 1358–1367.
- [134] M. Criado, A. Palomo, A. Fernández-Jiménez, P. Banfill, Alkali activated fly ash: effect of admixtures on paste rheology, *Rheol. Acta* 48 (2009) 447–455.
- [135] T. Bakharev, J.G. Sanjayan, Y.-B. Cheng, Effect of admixtures on properties of alkali-activated slag concrete, *Cement Concr. Res.* 30 (2000) 1367–1374.
- [136] A.I. Laskar, R. Bhattacharjee, Effect of plasticizer and superplasticizer on rheology of fly-ash-based geopolymers concrete, *ACI Mater. J.* 110 (2013).
- [137] A.M. Rashad, A comprehensive overview about the influence of different admixtures and additives on the properties of alkali-activated fly ash, *Mater. Des.* 53 (2014) 1005–1025.
- [138] J.G. Jang, N. Lee, H.-K. Lee, Fresh and hardened properties of alkali-activated fly ash/slag pastes with superplasticizers, *Construct. Build. Mater.* 50 (2014) 169–176.
- [139] F. Pacheco-Torgal, D. Moura, Y. Ding, S. Jalali, Composition, strength and workability of alkali-activated metakaolin based mortars, *Construct. Build. Mater.* 25 (2011) 3732–3745.
- [140] Y. Zaetang, A. Wongsa, P. Chindaprasirt, V. Sata, Utilization of crumb rubber as aggregate in high calcium fly ash geopolymers mortars, *J. GEOMATE* 17 (2019) 158–165.
- [141] T.M. Pham, Y.Y. Lim, M. Malekzadeh, Effect of pre-treatment methods of crumb rubber on strength, permeability and acid attack resistance of rubberised geopolymers concrete, *J. Build. Eng.* 41 (2021), 102448.
- [142] K. Arunkumar, M. Muthukannan, A.C. Ganesh, Mitigation of waste rubber tire and waste wood ash by the production of rubberized low calcium waste wood ash based geopolymers concrete and influence of waste rubber fibre in setting properties and mechanical behavior, *Environ. Res.* 194 (2021), 110661.
- [143] M. Balaha, A. Badawy, M. Hashish, Effect of Using Ground Waste Tire Rubber as Fine Aggregate on the Behaviour of Concrete Mixes, 2007.
- [144] A. Kashani, T.D. Ngo, P. Mendis, J.R. Black, A. Hajimohammadi, A sustainable application of recycled tyre crumbs as insulator in lightweight cellular concrete, *J. Clean. Prod.* 149 (2017) 925–935.
- [145] S. Guo, Q. Dai, R. Si, X. Sun, C. Lu, Evaluation of properties and performance of rubber-modified concrete for recycling of waste scrap tire, *J. Clean. Prod.* 148 (2017) 681–689.
- [146] N.F. Medina, R. Garcia, I. Hajirasouliha, K. Pilakoutas, M. Guadagnini, S. Raffoul, Composites with recycled rubber aggregates: properties and opportunities in construction, *Construct. Build. Mater.* 188 (2018) 884–897.
- [147] J. Sharp, E. Gartner, D. Macphee, Novel cement systems (sustainability). Session 2 of the fred glasser cement science symposium, *Adv. Cement Res.* 22 (2010) 195–202.
- [148] M. Dong, M. Elchalakani, A. Karrech, Development of high strength one-part geopolymers using sodium metasilicate, *Construct. Build. Mater.* 236 (2020), 117611.
- [149] S.N. Zamanabadi, S.A. Zareei, P. Shoaei, F. Ameri, Ambient-cured alkali-activated slag paste incorporating micro-silica as repair material: effects of alkali activator solution on physical and mechanical properties, *Construct. Build. Mater.* 229 (2019), 116911.
- [150] G.F. Huseien, A.R.M. Sam, K.W. Shah, J. Mirza, M.M. Tahir, Evaluation of alkali-activated mortars containing high volume waste ceramic powder and fly ash replacing GBFS, *Construct. Build. Mater.* 210 (2019) 78–92.
- [151] A. Wardhono, C. Gunasekara, D.W. Law, S. Setunge, Comparison of long term performance between alkali activated slag and fly ash geopolymers concretes, *Construct. Build. Mater.* 143 (2017) 272–279.
- [152] C. Bilim, O. Karahan, C.D. Atış, S. İlkkentapar, Influence of admixtures on the properties of alkali-activated slag mortars subjected to different curing conditions, *Mater. Des.* 44 (2013) 540–547.
- [153] S. Raffoul, R. Garcia, K. Pilakoutas, M. Guadagnini, N.F. Medina, Optimisation of rubberised concrete with high rubber content: an experimental investigation, *Construct. Build. Mater.* 124 (2016) 391–404.
- [154] T. Uygungölu, I.B. Topcu, The role of scrap rubber particles on the drying shrinkage and mechanical properties of self-consolidating mortars, *Construct. Build. Mater.* 24 (2010) 1141–1150.
- [155] B.H. Abdelaleem, M.K. Ismail, A.A. Hassan, The combined effect of crumb rubber and synthetic fibers on impact resistance of self-consolidating concrete, *Construct. Build. Mater.* 162 (2018) 816–829.
- [156] A. Sathonaowaphak, P. Chindaprasirt, K. Pimraksa, Workability and strength of lignite bottom ash geopolymers mortar, *J. Hazard Mater.* 168 (2009) 44–50.
- [157] P. Chindaprasirt, T. Chareerat, V. Sirivivatnanon, Workability and strength of coarse high calcium fly ash geopolymers, *Cement Concr. Compos.* 29 (2007) 224–229.
- [158] B. Muñoz-Sánchez, M.J. Arévalo-Caballero, M.C. Pacheco-Menor, Influence of acetic acid and calcium hydroxide treatments of rubber waste on the properties of rubberized mortars, *Mater. Struct.* 50 (2017) 1–16.
- [159] O. Youssif, M. Elchalakani, R. Hassanalı, R. Roychand, Y. Zhuge, R.J. Gravina, J. E. Mills, Mechanical performance and durability of geopolymers lightweight rubber concrete, *J. Build. Eng.* 45 (2022), 103608.
- [160] M. Valente, M. Sambucci, M. Chougan, S.H. Ghaffar, Reducing the emission of climate-altering substances in cementitious materials: a comparison between alkali-activated materials and Portland cement-based composites incorporating recycled tire rubber, *J. Clean. Prod.* 333 (2022), 130013.
- [161] G. Lazorenko, A. Kasprzhitskii, V. Mischninenko, Rubberized geopolymers composites: effect of filler surface treatment, *J. Environ. Chem. Eng.* 9 (2021), 105601.
- [162] Parveen Saloni, T.M. Pham, Y.Y. Lim, S.S. Pradhan, Jatin, J. Kumar, Performance of rice husk Ash-Based sustainable geopolymers concrete with Ultra-Fine slag and Corn cob ash, *Construct. Build. Mater.* 279 (2021), 122526.
- [163] S. Bate, Guide for structural lightweight aggregate concrete: report of ACI committee 213, *Int. J. Cem. Compos. Lightweight Concr.* 1 (1979) 5–6.
- [164] K. Somna, C. Jaturapitakkul, P. Kajitvichyanukul, P. Chindaprasirt, NaOH-activated ground fly ash geopolymers cured at ambient temperature, *Fuel* 90 (2011) 2118–2124.
- [165] S.A. Issa, M. Islam, M.A. Issa, A.A. Yousif, Specimen and aggregate size effect on concrete compressive strength, *Cem. Concr. Aggregates* 22 (2000) 103–115.
- [166] B. Zhang, Y. Feng, J. Xie, D. Lai, T. Yu, D. Huang, Rubberized geopolymers concrete: dependence of mechanical properties and freeze-thaw resistance on replacement ratio of crumb rubber, *Construct. Build. Mater.* 310 (2021), 125248.
- [167] Parveen Saloni, T.M. Pham, Y.Y. Lim, M. Malekzadeh, Effect of pre-treatment methods of crumb rubber on strength, permeability and acid attack resistance of rubberised geopolymers concrete, *J. Build. Eng.* 41 (2021), 102448.
- [168] S. Charkhtab Moghaddam, R. Madandoust, M. Jamshidi, I.M. Nikbin, Mechanical properties of fly ash-based geopolymers concrete with crumb rubber and steel fiber under ambient and sulfuric acid conditions, *Construct. Build. Mater.* 281 (2021), 122571.
- [169] A.M. Aly, M.S. El-Feky, M. Kohail, E.-S.A.R. Nasr, Performance of geopolymers concrete containing recycled rubber, *Construct. Build. Mater.* 207 (2019) 136–144.
- [170] J.C. Carroll, N. Helminger, Fresh and hardened properties of fiber-reinforced rubber concrete, *J. Mater. Civ. Eng.* 28 (2016), 04016027.
- [171] F. Hamidi, A. Valizadeh, F. Aslani, The Effect of Scoria, Perlite and Crumb Rubber Aggregates on the Fresh and Mechanical Properties of Geopolymer Concrete, Structures, Elsevier, 2022, pp. 895–909.
- [172] P. Nath, P.K. Sarker, Fracture properties of GGBFS-blended fly ash geopolymers cured in ambient temperature, *Mater. Struct.* 50 (2017) 1–12.
- [173] F. Aslani, F. Hamidi, A. Valizadeh, A.T.-N. Dang, High-performance fibre-reinforced heavyweight self-compacting concrete: analysis of fresh and mechanical properties, *Construct. Build. Mater.* 232 (2020), 117230.
- [174] I.I. Bashar, U.J. Alengaram, M.Z. Jumaat, A. Islam, H. Santhi, A. Sharmin, Engineering properties and fracture behaviour of high volume palm oil fuel ash based fibre reinforced geopolymers concrete, *Construct. Build. Mater.* 111 (2016) 286–297.
- [175] F. Hamidi, F. Aslani, Constitutive relationships for CNF-reinforced engineered cementitious composites and CNF-reinforced lightweight engineered cementitious composites at ambient and elevated temperatures, *Struct. Concr.* 21 (2020) 821–842.
- [176] F. Aslani, R. Jowkarimeimandi, Stress-strain model for concrete under cyclic loading, *Mag. Concr. Res.* 64 (2012) 673–685.

- [177] D. Grote, S. Park, M. Zhou, Dynamic behavior of concrete at high strain rates and pressures: I. experimental characterization, *Int. J. Impact Eng.* 25 (2001) 869–886.
- [178] M. Zhang, H. Wu, Q. Li, F. Huang, Further investigation on the dynamic compressive strength enhancement of concrete-like materials based on split Hopkinson pressure bar tests. Part I: Experiments, *Int. J. Impact Eng.* 36 (2009) 1327–1334.
- [179] A.C. 544, Guide to Design with Fiber-Reinforced Concrete, American Concrete Institute, 2018.
- [180] S. Erdem, A.R. Dawson, N.H. Thom, Microstructure-linked strength properties and impact response of conventional and recycled concrete reinforced with steel and synthetic macro fibres, *Construct. Build. Mater.* 25 (2011) 4025–4036.
- [181] L.-J. Hunag, H.-Y. Wang, Y.-W. Wu, Properties of the mechanical in controlled low-strength rubber lightweight aggregate concrete (CLSRLC), *Construct. Build. Mater.* 112 (2016) 1054–1058.
- [182] A.M. Neville, Properties of Concrete, Longman, London, 1995.
- [183] S.T. Lee, H.Y. Moon, R.N. Swamy, Sulfate attack and role of silica fume in resisting strength loss, *Cement Concr. Compos.* 27 (2005) 65–76.
- [184] M. Nuzaimah, S.M. Sapuan, R. Nadlene, M. Jawaid, Effect of surface treatment on the performance of polyester composite filled with waste glove rubber crumbs, *Waste and Biomass Valorization* 12 (2021) 1061–1074.
- [185] M. Nuzaimah, S.M. Sapuan, R. Nadlene, M. Jawaid, Sodium hydroxide treatment of waste rubber crumb and its effects on properties of unsaturated polyester composites, *Appl. Sci.* 10 (2020) 3913.
- [186] G. Lazorenko, A. Kasprzhitskii, A. Kruglikov, V. Mischinenko, V. Yavna, Sustainable geopolymer composites reinforced with flax tows, *Ceram. Int.* 46 (2020) 12870–12875.
- [187] G. Lazorenko, A. Kasprzhitskii, V. Yavna, V. Mischinenko, A. Kukharskii, A. Kruglikov, A. Kolodina, G. Yalovega, Effect of pre-treatment of flax tows on mechanical properties and microstructure of natural fiber reinforced geopolymer composites, *Environ. Technol. Innovat.* 20 (2020), 101105.
- [188] M. Amran, S. Debbarma, T. Ozbakaloglu, Fly ash-based eco-friendly geopolymer concrete: a critical review of the long-term durability properties, *Construct. Build. Mater.* 270 (2021), 121857.
- [189] X.Y. Zhuang, L. Chen, S. Komarneni, C.H. Zhou, D.S. Tong, H.M. Yang, W.H. Yu, H. Wang, Fly ash-based geopolymers: clean production, properties and applications, *J. Clean. Prod.* 125 (2016) 253–267.
- [190] P. Duxson, J.L. Provis, G.C. Luke, F. Separovic, J.S. van Deventer, 29Si NMR study of structural ordering in aluminosilicate geopolymer gels, *Langmuir* 21 (2005) 3028–3036.
- [191] J. Davidovits, Geopolymers: ceramic-like inorganic polymers, *J. Ceram. Sci. Technol* 8 (2017) 335–350.
- [192] Z. Li, R. Chen, L. Zhang, Utilization of chitosan biopolymer to enhance fly ash-based geopolymers, *J. Mater. Sci.* 48 (2013) 7986–7993.
- [193] T. Huang, Z. Sun, Advances in multifunctional graphene-geopolymer composites, *Construct. Build. Mater.* 272 (2021), 121619.
- [194] O. Ünal, T. Uygunoglu, A. Yıldız, Investigation of properties of low-strength lightweight concrete for thermal insulation, *Build. Environ.* 42 (2007) 584–590.
- [195] G.J. Gluth, W.D. Rickard, S. Werner, S. Pirsikawetz, Acoustic emission and microstructural changes in fly ash geopolymers exposed to simulated fire, *Mater. Struct.* 49 (2016) 5243–5254.
- [196] N.A. Jaya, L. Yun-Ming, H. Cheng-Yong, M.M.A.B. Abdullah, L.F. Wah, O. Wan-En, I.M.Z. Abidin, N. Azaman, Effect of anisotropic pores on the material properties of metakaolin geopolymers incorporated with corrugated fiberboard and rubber, *J. Mater. Res. Technol.* 14 (2021) 822–834.
- [197] H. Yangthong, S. Wisunthorn, S. Pichaiyut, C. Nakason, Novel epoxidized natural rubber composites with geopolymers from fly ash waste, *Waste Manag.* 87 (2019) 148–160.
- [198] E. Adesanya, K. Ohenoja, T. Luukkonen, P. Kinnunen, M. Illikainen, One-part geopolymers cement from slag and pretreated paper sludge, *J. Clean. Prod.* 185 (2018) 168–175.
- [199] Z. Abdollahnejad, T. Luukkonen, M. Mastali, C. Giosue, O. Favoni, M. Ruello, P. Kinnunen, M. Illikainen, Microstructural analysis and strength development of one-part alkali-activated slag/ceramic binders under different curing regimes, *Waste and Biomass Valorization* 11 (2020) 3081–3096.
- [200] S.M.A. Qaidi, Ultra-high-performance Fiber-Reinforced Concrete: Challenges, 2022.
- [201] S.M.A. Qaidi, Ultra-high-performance Fiber-Reinforced Concrete: Applications, 2022.
- [202] S.M.A. Qaidi, Ultra-high-performance Fiber-Reinforced Concrete: Cost Assessment, 2022.
- [203] H. Abdel-Gawwad, K.A. Khalil, Application of thermal treatment on cement kiln dust and feldspar to create one-part geopolymer cement, *Construct. Build. Mater.* 187 (2018) 231–237.
- [204] J. Ren, L. Zhang, R. San Nicolas, Degradation process of alkali-activated slag/fly ash and Portland cement-based pastes exposed to phosphoric acid, *Construct. Build. Mater.* 232 (2020), 117209.
- [205] T. Bakharev, J.G. Sanjayan, Y.-B. Cheng, Resistance of alkali-activated slag concrete to acid attack, *Cement Concr. Res.* 33 (2003) 1607–1611.
- [206] S.M.A. Qaidi, Ultra-high-performance Fiber-Reinforced Concrete: Hydration and Microstructure, 2022.
- [207] S.M.A. Qaidi, Ultra-high-performance Fiber-Reinforced Concrete: Mixture Design, 2022.
- [208] S.M.A. Qaidi, Ultra-high-performance Fiber-Reinforced Concrete: Principles and Raw Materials, 2022.
- [209] S.M.A. Qaidi, PET-concrete Confinement with CFRP, 2021.
- [210] S.M.A. Qaidi, PET-Concrete, 2021.
- [211] A.O. Atahan, U.K. Sevim, Testing and comparison of concrete barriers containing shredded waste tire chips, *Mater. Lett.* 62 (2008) 3754–3757.
- [212] S. Saheed, Y.M. Amran, M. El-Zeadani, F.N.A. Aziz, R. Fediu, R. Alyousef, H. Alabduljabbar, Structural behavior of out-of-plane loaded precast lightweight EPS-foam concrete C-shaped slabs, *J. Build. Eng.* 33 (2021), 101597.
- [213] A. Senate, Retirement of Coal Fired Power Stations: Final Report to the Environment and Communications References Committee, Parliament House, Canberra, 2017.
- [214] Y.M. Amran, M. El-Zeadani, Y.H. Lee, Y.Y. Lee, G. Murali, R. Fediu, Design Innovation, Efficiency and Applications of Structural Insulated Panels: A Review, Elsevier, 2020, pp. 1358–1379.
- [215] S.M.A. Qaidi, Ultra-high-performance Fiber-Reinforced Concrete: Durability Properties, 2022.
- [216] S.M.A. Qaidi, Ultra-high-performance Fiber-Reinforced Concrete: Hardened Properties, 2022.
- [217] S.M.A. Qaidi, Ultra-high-performance Fiber-Reinforced Concrete: Fresh Properties, 2022.
- [218] A. Mujdeci, D. Bompá, A. Elghazouli, Confinement effects for rubberised concrete in tubular steel cross-sections under combined loading, *Arch. Civ. Mech. Eng.* 21 (2021) 1–20.
- [219] H. Thilakarathna, D. Thambiratnam, M. Dhanasekar, N. Perera, Numerical simulation of axially loaded concrete columns under transverse impact and vulnerability assessment, *Int. J. Impact Eng.* 37 (2010) 1100–1112.
- [220] O. Youssif, R. Hassanli, J.E. Mills, Mechanical performance of FRP-confined and unconfined crumb rubber concrete containing high rubber content, *J. Build. Eng.* 11 (2017) 115–126.
- [221] M. Valente, M. Sambucci, A. Sibai, Geopolymers vs. Cement matrix materials: how nanofiller can help a sustainability approach for smart construction applications—a review, *Nanomaterials* 11 (2021) 2007.
- [222] S.G. Maxineasa, K. Neocleous, L. Dumitrescu, K. Themistocleous, N. Tarau, D. G. Hadjimitsis, Environmental LCA of Innovative Reuse of All End-Of-Life Tyre Components in Concrete, 2017.
- [223] M. Medine, H. Trouzine, J.B. de Aguiar, H. Djadouni, Life cycle assessment of concrete incorporating scrap tire rubber: comparative study, *Nature & Technology* (2020) 1–11.
- [224] C. Ouellet-Plamondon, G. Habert, Life Cycle Assessment (LCA) of Alkali-Activated Cements and Concretes, *Handbook of Alkali-Activated Cements, Mortars and Concretes*, Elsevier, 2015, pp. 663–686.
- [225] B.C. McLellan, R.P. Williams, J. Lay, A. Van Riessen, G.D. Corder, Costs and carbon emissions for geopolymers pastes in comparison to ordinary portland cement, *J. Clean. Prod.* 19 (2011) 1080–1090.
- [226] J. Shang, J.-G. Dai, T.-J. Zhao, S.-Y. Guo, P. Zhang, B. Mu, Alteration of traditional cement mortars using fly ash-based geopolymers modified by slag, *J. Clean. Prod.* 203 (2018) 746–756.